Environmental Science & Technology

Critical Review

pubs.acs.org/est

Inherent Tracers for Carbon Capture and Storage in Sedimentary Formations: Composition and Applications

Stephanie Flude,*[,†,‡] Gareth Johnson,[†] Stuart M. V. Gilfillan,[†] and R. Stuart Haszeldine[†]

[†]School of Geosciences, The University of Edinburgh, Grant Institute, King's Buildings, James Hutton Road, Edinburgh EH9 3FE, U.K.

[‡]Isotope Geosciences Unit, Scottish Universities Environmental Research Centre, Rankine Avenue, East Kilbride G75 0QF, U.K.

Supporting Information

ABSTRACT: Inherent tracers—the "natural" isotopic and trace gas composition of captured CO_2 streams—are potentially powerful tracers for use in CCS technology. This review outlines for the first time the expected carbon isotope and noble gas compositions of captured CO_2 streams from a range of feedstocks, CO_2-generating processes, and carbon capture techniques. The C-isotope composition of captured CO_2 will be most strongly controlled by the feedstock, but significant isotope fractionation is possible during capture; noble gas concentrations will be controlled by the capture technique employed. Comparison with likely baseline data suggests that CO_2 generated from fossil fuel feedstocks will often have $\delta^{13}C$ distinguishable from storage reservoir CO_2. Noble gases in amine-captured CO_2 streams are likely to be low concentration, with isotopic ratios dependent on the feedstock, but CO_2 captured from oxyfuel plants may be strongly enriched in Kr and Xe which are potentially valuable subsurface tracers. CO_2 streams derived from fossil fuels will have noble gas isotope ratios reflecting a radiogenic component that will be difficult to distinguish in the storage reservoir, but inheritance of radiogenic components will provide an easily recognizable signature in the case of any unplanned migration into shallow aquifers or to the surface.

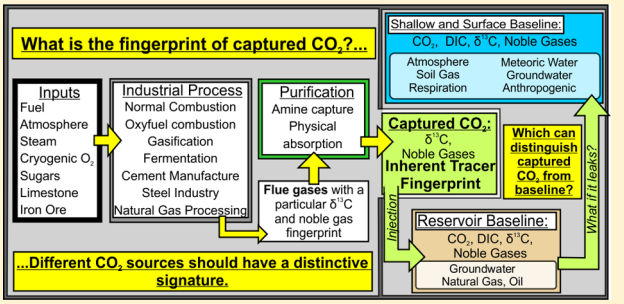

1. INTRODUCTION

1.1. Need for CCS. The link between atmospheric concentrations of anthropogenically produced CO_2 and global warming is unequivocal,[1−4] and CO_2 emissions must be drastically reduced, and eventually stopped, if we are to avoid catastrophic, irreversible climate change. Carbon capture and storage (CCS) features prominently in all scenarios that consider timely and feasible reductions in CO_2 emissions.[1,5] Importantly, CCS is the only technology that can substantially reduce carbon emissions from industrial processes such as chemical synthesis and steel production. Climate models are increasingly relying on the use of negative emissions to limit global average temperature rise to 2 °C and include large amounts of bioenergy combined with CCS (BECCS), as this is the only feasible, industrial-scale negative emissions technology currently available.[6]

Carbon capture in the context of this review involves removal of CO_2 from the flue gases of point-source emitters, such as power stations and industrial plants, to produce a stream of high concentration CO_2. Current well-developed capture techniques are often classified into one of three categories. (1) "Amine capture", also referred to as "post-combustion capture" because it was originally envisaged to be applied most often to fossil fuel or biomass combustion-fired power stations, removes CO_2 from a gas stream by chemical reaction of the CO_2 with an amine solvent (with or without the use of membranes) and is already widely used by the hydrocarbon industry to remove CO_2 from produced natural gas.[7] (2) "Oxycombustion" or "oxyfuel combustion" produces a high CO_2 purity flue gas by burning fuel in an oxygen-rich atmosphere, rather than air, and recycling the flue gas into the combustion chamber. (3) "Pre-combustion capture" collects the CO_2 produced during gasification processes and is so named for the potential to generate hydrogen fuel, which can be combusted without producing CO_2 to produce electricity. These general carbon capture terms were developed in the context of CCS being most readily applied to electricity generation (hence the focus on pre- or post-combustion). In reality, these capture techniques are already applied to a much wider range of industrial activities, such as natural gas processing, synfuel production, and chemical/fertilizer manufacture (see Section 3), so classification according to the stage of electricity generation is no longer appropriate. As such, we use the terms "amine capture", "oxyfuel" and "gasification" when discussing these three different types of capture technique. Additional pressure-based adsorption techniques onto solid adsorbents (e.g., pressure-swing adsorption) or

Received: March 29, 2016
Revised: June 30, 2016
Accepted: July 5, 2016
Published: July 5, 2016

organic solvents are also used during gas purification, especially as part of the gasification processes.

The efficiency of CO_2 capture and the purity of the captured CO_2 stream vary between ~95% and 99.9%[2,8] depending on the capture method, post-capture cleanup, and specific conditions employed. Industrial specifications require a CO_2 purity of >95% for transport and storage, to maximize density and avoid problematic phase changes, so end-product CO_2 streams tend to contain 90−99% CO_2, with minor to trace amounts of N_2, hydrocarbons, H_2S, NO_X, SO_X, O_2, H_2O, and noble gases (especially Ar).[7−9]

1.2. Need for CO_2 Tracers. Commercial-scale carbon-storage projects will be required by governmental regulatory bodies to monitor CO_2 injected for storage and mitigate any unplanned behavior, such as migration out of the storage reservoir (leakage) or to the surface (seepage), in the storage complex.[10] Furthermore, being able to trace the migration and reactions of injected CO_2 in the subsurface is fundamental to the continual assessment of injectivity, identification of CO_2 trapping mechanisms, and quantification of storage capacity, all of which need to be well-understood and characterized to ensure storage security. Geophysical techniques, while useful monitoring tools, remain limited in their ability to quantify CO_2 pore space saturation and dissolution at high spatial resolution.[11−13] Seepage rates of 0.001−0.01% per year are generally considered acceptable on a climate accounting basis, amounting to a loss of ~1% of the injected CO_2 over 100 years, a target adopted by the U.S. Department of Energy.[14,15] Conclusive detection of such seepage rates by measurement of CO_2 concentrations remains problematic due to natural background CO_2 fluctuations. A potential solution to this problem is the use of geochemical tracers, detectable at low concentrations due to their low background level in the atmosphere or storage complex. Addition of geochemical tracers for environmental monitoring and interpretation of reservoir dynamics is a long-standing practice in the hydrocarbon industry, with perfluorocarbon tracer compounds (PFTs),[16] tritiated and perdeuterated CH_4 and H_2O, freons, sulfur hexafluoride (SF_6)[17] and noble gases such as Kr and Xe[18] proving to be particularly useful tracers.

Tracers can be classified in terms of their relationship to the injected CO_2 as (1) added tracers (substances added to the CO_2 stream prior to injection, e.g., SF_6), (2) inherent or natural tracers (substances already present in the CO_2 stream or the isotopic composition of the CO_2 itself), or (3) indirect tracers (changes to baseline values resulting from interaction of the CO_2 with the natural environment, e.g., pH or cation content due to mineral dissolution).[19] Adding geochemical tracers to injected CO_2 can facilitate detailed monitoring and modeling of CO_2 storage, but concerns remain regarding the economic cost of tracers in commercial-scale storage sites, the possibility of increased background (lower sensitivity)/site contamination, and the environmental impact of such compounds.[17,20−22] PFTs and SF_6, in particular, are potent greenhouse gases with atmospheric residence times of 1000s of years.[17,22]

Using the isotopic and trace element geochemistry of the injected CO_2 itself as a tracer has the potential to facilitate in-reservoir tracing and leakage monitoring with minimal economic and environmental impact compared with added tracers. Furthermore, Article 12.1 of the EU directive on CCS states that "no waste or other matter may be added for the purpose of disposing of [the CO_2]";[10] while provision has been made in the directive for allowing the addition of tracers, these require consideration on a case-by-case basis, so use of inherent CO_2 tracers may help to simplify applications for CO_2-storage permits.

Here, we describe the inherent tracers which will be most useful for fingerprinting and monitoring CO_2 during storage, summarize the currently available information regarding inherent tracer signatures in both captured CO_2 and potential storage reservoirs, and highlight the further research necessary to facilitate the application of inherent tracer geochemistry to CCS. As we will show, the feasibility of using inherent tracers for measuring, monitoring, and verification (MMV) depends on a number of variables, including the baseline composition of reservoirs and overburden of interest and the inherent tracer composition of the captured CO_2 stream. These will vary extensively depending on a number of factors, and hence specific discussion of detection limits of the inherent tracers we describe is out of the scope of this review.

2. INHERENT TRACERS

For tracers to be effective, their compositions must be distinct from that of the storage site, including the host reservoir, overburden, and local atmosphere. In this section we provide a brief background to and highlight further information on the isotope and trace gas systems that may be used as inherent tracers.

2.1. CO_2 Isotopic Composition. The stable isotopes of C and O of injected CO_2 are an obvious potential tracer and have been successfully used in a number of projects to identify CO_2 migration and quantify pore space saturation and dissolution of CO_2 (see section 6). Much of this work and background theory relevant to CCS have recently been summarized in a number of review papers.[12,19,23−26] However, the isotopic composition of the captured CO_2 itself has received less attention, which we address in section 3. For this review, we concentrate on using C-isotopes as a means of fingerprinting the injected CO_2. While O-isotopes of captured CO_2 may be a useful, quantitative monitoring tool,[11] rapid equilibration of O-isotopes between CO_2 and water[27] means that the O-isotope composition of CO_2 will be controlled by any volumentrically significant water it interacts with; as a result the O-isotope composition of CO_2 is expected to change significantly after injection into the storage reservoir and so not provide a diagnostic tracer of the CO_2 itself. Hence O-isotopes are not discussed in detail in this review.

For context, the range of isotopic compositions occurring in nature are shown in Figure 1 with details provided in Supporting Information Table S1. C-isotope values are presented in $\delta^{13}C$ relative to Vienna Pee Dee Belemnite (V-PDB), where

$$\delta^{13}C/‰ = \left(\frac{(^{13}C/^{12}C)_{sample}}{(^{13}C/^{12}C)_{reference}} - 1 \right) \times 1000$$

Isotope fractionation, enrichment factors (ε), and conversion between isotopic values relative to different standards are covered in detail in recent review papers which we refer interested readers to.[12,19,23−26]

2.2. Noble Gases. Noble gases (He, Ne, Ar, Kr, and Xe) are particularly useful for tracing interaction of gases with fluids due to their unreactive nature and Henry's Law controlled solubility; in general, solubility increases with elemental mass and decreases with increasing temperature. Noble gases will preferentially partition into gas > oil > fresh water > saline

DOI: 10.1021/acs.est.6b01548
Environ. Sci. Technol. 2016, 50, 7939−7955

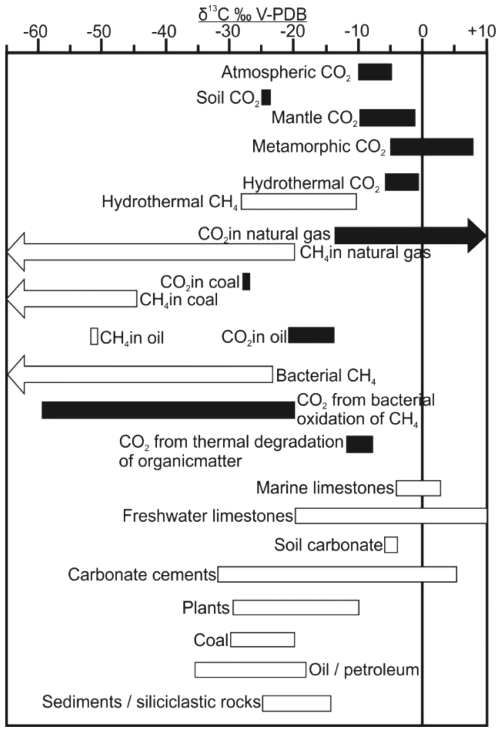

Figure 1. C-isotope values for a range of naturally occurring materials. Black boxes indicate CO_2. White boxes are other substances. Arrows represent values off the scale of the diagram. See Supporting Information Table S1 for references. Note that a wide range of $\delta^{13}C$ values are covered by naturally occurring CO_2 sources.

water, so mixing and migration of different fluids and gases in the subsurface may lead to multiple re-equilibration events that result in elemental fractionation of the noble gases.[28,29] Hence, noble gases are being increasingly used to identify and quantify hydrocarbon migration pathways from modeling the elemental fractionation that occurs during partitioning between water, oil, and gas.[30,32] Noble gases in the subsurface can be considered a mixture of three components:[33] (1) atmospheric derived noble gases, introduced to the subsurface by equilibration with meteoric water and recharge; (2) radiogenic noble gases produced in situ by decay of radioactive elements; (3) terrigenic fluids originating from defined geochemical reservoirs. Two common terrigenic components in sedimentary formations are crust and mantle. Mantle noble gases are enriched in ^3He, with $^3He/^4He$ as high as 70 R_A (R_A being $^3He/^4He$ of atmosphere, 1.339×10^{-6}) while crustal noble gases are enriched in radiogenic noble gases (^4He and ^{40}Ar) and have $^3He/^4He < 0.7$ R_A[32]. In subsurface fluids a distinction exists between radiogenic and crustal components; the terrigenic crustal component is derived from radioactive decay, but represents the cumulative accumulation in the host rock, and is thus controlled by the age and chemistry of the geological formation hosting the fluid and the openness of the system, while the radiogenic component is added to the fluid by in situ radioactive decay and is thus a function of the host formation chemistry and fluid residence time.[33] Summaries of noble gas data relevant to CCS are shown in Table 1.

3. GEOCHEMISTRY OF THE CAPTURED CO_2 STREAM

Two sources of information are available to assess the likely composition of the captured CO_2 stream: (1) a limited number of direct measurements on captured CO_2 and (2) hypothetical considerations of the feedstocks and processes involved in CO_2 generation. We analyze this information to draw conclusions about the range of CO_2 compositions that can be expected for different feedstocks and processes, which are summarized in Table 2. Further information regarding $\delta^{13}C$ and noble gas content of a range of relevant feedstocks are provided in the Supporting Information.

3.1. Direct Measurement of the Captured CO_2 Stream. CCS projects have reported captured CO_2 stream data from two oxycombustion plants, three synfuel/hydrogen production plants, two fertilizer manufacturers, one natural gas processing plant, and one unknown combustion source. $\delta^{13}C$ has been the most widely analyzed tracer in captured CO_2 to date, giving a wide range of values from −51 to −4.7‰. Limited noble gas data are available for CO_2 streams from fertilizer and oxyfuel plants. The limited available data is consistent with theoretical considerations discussed below, but the uncertainties involved (most often relating to the precise feedstock composition) hinder robust predictions of captured CO_2 stream chemistry, and more studies are needed to clarify the $\delta^{13}C$ of captured CO_2.

3.2. Fuel Combustion for Energy Production. Power stations are some of the largest point sources of CO_2 emissions in the developed world, making them obvious targets for CCS. In most cases, power is generated by combustion of material, often fossil fuels but with an increasing use of biomass, to drive a turbine and generate electricity. Capture of combustion-produced CO_2 will be either via amine capture or oxyfuel methods.

3.2.1. Carbon Isotopes. For CO_2 derived from fossil fuel combustion, Widory[34] identified ^{13}C depletion in the CO_2

Table 1. Summary of Noble Gas Concentrations and Solubilities

	air (ppbv)[a]	water (ppbv)[b]	oil (mol ppb)	gas (mol ppb)	solubility in water[g]	solubility in oil[g]
^4He	5,240	50	12,000−130,000[c]	580−3,838,000[e,f]	0.0090	0.0211
^{20}Ne	18,180	181	2−21[c]	4.1−1,294.4[e,f]	0.0096	0.0198
^{40}Ar	9,340,000	398,400	10,700−26,900[c]	51,100−208,300[6]	0.036	0.0158
^{36}Ar	31,607	1,348	1−151[d]	20−11,849[e,f]		
^{84}Kr	650	51		1.6−120[e,f]	0.0388	0.400
^{136}Xe	8	0.9		0.1−5.7[e,f]	0.0603	1.080

[a]Calculated from Porcelli et al.[105] [b]Based on calculated equilibrium concentrations of elemental noble gases in low salinity water at 10 °C from Lake Baikal,[33] using the simplified assumption that 1 g of water = 1 cm^3, and converted to isotopic abundances using isotopic ratios from Porcelli et al.[105] [c]Calculated from Ballentine et al.[86] [d]Calculated from Torgersen and Kennedy.[88] [e]Calculated from Prinzhofer et al.[130] [f]Calculated from Kotarba et al.[131] [g]Solubilities[130] expressed as the ratio of the noble gas concentration in the liquid to the concentration in the gas (mol m^{-3}/mol m^{-3}), at 50 °C and atmospheric pressure for water and heavy (API 25) oil.

DOI: 10.1021/acs.est.6b01548
Environ. Sci. Technol. 2016, 50, 7939−7955

Table 2. Expected Carbon Isotope and Noble Gas Compositions of the CO_2 Stream Generated by a Variety of Industrial and Energy-Generating Technologies, Relative to Their Source Components (Feedstock, Combustion Atmosphere, etc.) and with Likely Fractionations Where Relevant[a]

Process	Feedstock	$\delta^{13}C$ ‰ V-PDB of feedstock	$\delta^{13}C$ Ɛ ‰ of process	$\delta^{13}C$ of CO_2 ‰ V-PDB	Noble gas content of components	Noble Gases in CO_2
Normal Combustion *	Coal	-30 to -20	-1.3	-31.3 to -21.3	High ^{4}He and ^{40}Ar in fossil fuels. Atmospheric noble gases from air.	Air-like, plus enriched ^{4}He and ^{40}Ar.
	Oil	-36 to -18		-37.3 to -19.3		
	Natural Gas	<-60 to -20		<-61 to -21.3		
	C3 biomass	-30 to -24	0	-30 to -24	Atmospheric noble gases	Air-like noble gases
	C4 biomass	-15 to -10	0 to +4	-15 to -6		
Oxyfuel	Coal	-30 to -20	-1.3	-31.3 to -21.3	High ^{4}He and ^{40}Ar in fossil fuels. Heavy noble gases in cryogenic oxygen.	Enriched in heavy noble gases, ^{4}He and ^{40}Ar.
	Oil	-36 to -18	-1.3	-37.3 to -19.3		
	Natural Gas	<-60 to -20	-1.3	<-61 to -21.3		
	C3 biomass	-30 to -24	0	-30 to -24	Heavy noble gases in cryogenic oxygen.	Enriched in heavy noble gases.
	C4 biomass	-15 to -10	0 to +4	-15 to -6		
Gasification / Syngas	Coal	-30 to -20	Difficult to predict. Possible small –ve Ɛ	<-30 to <-20	High ^{4}He and ^{40}Ar in fossil fuels. Use of steam will add atmospheric noble gases. Use of cryogenic O_2 will add heavy noble gases.	Atmospheric noble gases. Possibly enriched in heavy noble gases. High ^{4}He and ^{40}Ar for fossil fuel feedstocks.
	Oil	-36 to -18		<-36 to < -18		
	Natural Gas	<-60 to -20		<-60 to < -20		
	C3 biomass	-30 to -24		<-30 to <-24		
	C4 biomass	-15 to -10		<-15 to <-10		
Synfuel / chemical plant	Coal	-30 to -20	Possible small +ve Ɛ	>-30 to >-20	Increased likelihood of using cryogenic O_2 will add heavy noble gases	Air like ratios and likely enriched in heavy noble gases
	Oil	-36 to -18		>-36 to > -18		
	Natural Gas	<-60 to -20		>-60 to > -20		
Fermentation	C4 Sugars	-15 to -10	+4 to +6	-11 to -4	Air saturated water	Air-like ratios, depleted concentrations relative to air.
Cement *	Coal + Limestone	-30 to -20 0	-1.3 for coal + mixing	-16 to -11	High ^{4}He and ^{40}Ar in fossil fuels. Atmospheric noble gases from air. Heavy noble gas enrichment for oxyfuel.	Air-like, plus enriched ^{4}He and ^{40}Ar. Heavy noble gas enrichment for oxyfuel.
Steel Industry: ISP *	Coal	-30 to -20	-1.3	-31.3 to -21.3	High ^{4}He and ^{40}Ar in fossil fuels. Atmospheric noble gases from air.	Air-like, plus enriched ^{4}He and ^{40}Ar.
Steel Industry: DRI	As for Syngas Iron ore	As for Syngas			High ^{4}He and ^{40}Ar in iron oxide. Atmospheric noble gases from air. Heavy noble gases in cryogenic oxygen?	Air-like, plus enriched ^{4}He and ^{40}Ar. Possibly enriched in heavy noble gases.
Natural gas processing (Amine capture)	CO_2 co-existing with natural gas	-14 to +14	-20 to +2.5	-34 to +21	High ^{4}He and ^{40}Ar in natural gas.	Noble gases likely lost during capture. Preferential retention of heavy noble gases. Radiogenic and terrigenic isotope ratios retained but abundances << air.

[a]Subsequent amine capture or physical absorption are not included. For processes that will be followed with amine capture (* in "process" column), add $\delta^{13}C$ enrichment of −20 to +2.5‰ and depletion of noble gas concentrations (especially light noble gases). For physical absorption in organic solvents (may or may not be used with all other processes), add a small positive C-isotopic enrichment, dependent on the relative efficiencies of the absorption and desorption processes, and depletion of noble gas concentrations (especially light noble gases). References for the C-isotope composition of feedstock and other components are given in the text and in the Supporting Information tables, and values are summarised in Figure 1.

relative to the fuel, amounting to $\delta^{13}C \sim -1.3$‰ for a range of fossil fuel types (solid, liquid, and gas). More recent work has measured $\delta^{13}C$ during coal combustion and found that resulting CO_2 has $\delta^{13}C$ between −2.39 and +2.33‰ relative to the coal feedstock.[35] $\delta^{13}C_{CO_2}$ of −46.2‰[36] has been reported for CO_2 derived from combustion of natural gas, which is consistent with (the admittedly wide range of) expected values (Figure 1), but the capture method was not reported.

For biomass, complete combustion of C3 and C4 plants produces CO_2 with the same C-isotope composition of the bulk plant, but partial combustion of C4 plants may result in ^{13}C enrichment of the CO_2 (up to +4‰ at 3% combustion).[37] The C-isotope signature of CO_2 produced by burning biomass will therefore depend on the specific feedstock and the efficiency of the combustion process. Given the higher temperatures associated with oxycombustion, we might expect a higher efficiency of biomass combustion compared to normal combustion, so no isotopic fractionation would be expected. Reported $\delta^{13}C$ of CO_2 from oxycombustion of natural gas (−40‰, Rousse CCS project[38]) and lignite (−26‰, Ketzin CCS project; see Supporting Information Table S2) are consistent with expected values (−61 to −21.3‰ and −31.3 to −21.3‰, respectively; Table 2).

3.2.2. Noble Gases. To the best of our knowledge, very little data are available on the noble gas content of combustion gases. Noble gases in combustion flue gases will be derived from the material being combusted and from the combustion atmosphere (air for normal combustion; cryogenic oxygen for oxyfuel). Concentrations of most noble gases in hydrocarbons are generally 2−3 orders of magnitude lower than in air (Table 1), so atmospheric noble gases are expected to dominate. A radiogenic or terrigenic isotopic component might be

DOI: 10.1021/acs.est.6b01548
Environ. Sci. Technol. 2016, 50, 7939−7955

resolvable in hydrocarbon derived CO_2 due to elevated ^4He in fossil fuels.

For oxyfuel, additional heavy noble gases (Ar, Kr, and Xe) may be introduced with the cryogenically purified O_2. CO_2 injected at the Rousse CCS project was derived from oxycombustion of natural gas.[38] The source natural gas fuel was enriched in ^4He and depleted in ^{20}Ne, ^{36}Ar, ^{40}Ar, and ^{84}Kr relative to air;[38] the resulting CO_2 remained enriched in ^4He and depleted in ^{20}Ne relative to air, but Ar isotopes had concentrations similar to air and ^{84}Kr was enriched by an order of magnitude compared to air.[38] Enrichments of Ar (up to 2%) in oxyfuel-captured CO_2 have also been observed during oxyfuel pilot experiments,[8] despite distillation procedures designed to remove inert gases.[7]

3.3. Gasification Processes/Synfuel Production/Pre-combustion CO_2 Capture. Here we use the term "gasification processes" to refer to the range of reactions used to generate Syngas (H_2 and CO) from a variety of fuel stocks. Syngas can be further processed by Fischer–Tropsch reactions to create a range of chemicals and synthetic fuels (synfuels), including synthetic natural gas (SNG) and Fischer–Tropsch liquid fuels. These chemical reactions are described in the Supporting Information.

Syngas is generated by a two stage chemical reaction. At the first stage, carbon monoxide (CO) and H_2 are produced from the feedstock, via either steam reforming or partial oxidation, followed by addition of steam to stimulate a "shift reaction" that converts CO to CO_2, generating more H_2.[7] For synfuel production the syngas stream is passed through a synthesis reactor where CO and H_2 are catalytically converted to the desired chemical.[7] CO_2 from the entire process is captured both upstream and downstream of the synthesis reactor and the captured CO_2 will be a combination of CO_2 generated from different gasification stages, with a decreased input from the shift reaction as CO is used in Fischer–Tropsch reactions. The resulting CO_2 is removed from the gas stream by either chemical solvents (e.g., amine capture) or physical solvents (e.g., cold methanol).[7]

3.3.1. Carbon Isotopes. Fractionation of C-isotopes during gasification is likely due to increased bond strength of $^{13}C–^{12}C$ compared to $^{12}C–^{12}C$, resulting in ^{13}C depletion in low molecular weight gases and ^{13}C enrichment in heavy residues such as tar and vacuum bottoms.[39] C-isotope ratios will be $\delta^{13}C_{CO} < \delta^{13}C_{CH4} < \delta^{13}C_{hydrocarbons} < \delta^{13}C_{coal} < \delta^{13}C_{char} < \delta^{13}C_{CO_2}$ at typical gasification temperatures (>1000 °C).[40−42] This suggests that any CO_2 produced by incomplete reactions in the first stage of gasification is likely to be enriched in ^{13}C compared to the original feedstock, while the resulting CO will be depleted in ^{13}C. This agrees with experimental results from underground coal gasification plants,[39,41,43] and natural gas generation via pyrolysis of coal and lignite,[44,45] which produced CO_2 enriched in ^{13}C by 2−10‰ relative to the feedstock. Conversely, CO_2 generated from CO via the shift reaction will be depleted in ^{13}C. In a simplistic scenario, all CO_2 resulting from gasification will be derived from the shift reaction, so we could expect CO_2 captured from Syngas plants to be the same as or isotopically lighter than the feedstock, depending on the efficiency of the gasification reactions and proportion of feedstock not converted to Syngas. For synfuel and F-T plants, the ^{13}C-depleted CO will be used in chemical synthesis, so early generated, CO_2 slightly enriched in ^{13}C will dominate. In reality, gasification of solid fuels is likely to produce CO_2 and CH_4 in addition to CO and H_2, so the isotopic composition of resulting CO_2 will depend on the proportions of ^{13}C-enriched, early produced CO_2 and ^{13}C-depleted, shift-reaction CO_2. It is thus difficult to precisely predict the C-isotopic composition of CO_2 captured from syngas and synfuel plants. However, it is likely that the various fractionation and mixing processes will average out, giving CO_2 with an isotopic composition similar to or slightly more ^{13}C-depleted than the feedstock for syngas plants, and similar to or slightly more ^{13}C-enriched than the feedstock for chemical and synfuel plants.

One of the sources of CO_2 injected at the Ketzin project was reportedly a byproduct of hydrogen production[46] at an oil refinery.[47] This CO_2 has $\delta^{13}C \sim -30.5‰$[47] (Table S2) which is indistinguishable from the range of $\delta^{13}C$ values expected for oil (−18 to −36 ‰, Table 2). CO_2 injected in the Frio project was derived from a refinery in Bay City, TX, USA, and the Donaldsonville fertilizer plant, Louisiana.[48] Reported $\delta^{13}C$ of the injected CO_2 was −51 to −35‰.[49] While the end-member $\delta^{13}C$ compositions were not reported, the values are consistent with those for natural gas (fertilizer plant) and oil (refinery) (see Table 2 and Figure 1). CO_2 captured from the Scotford Bitumen Upgrader, Canada, was derived from hydrogen production and purified using amine capture;[50] most hydrogen production in the region is produced using steam methane reforming.[51] The captured CO_2 has $\delta^{13}C$ of −37‰,[52] which is within the range of $\delta^{13}C$ values for natural gas. While the range of possible feedstock compositions is too wide to be conclusive, these data are consistent with our above predictions. The CO_2 injected at Weyburn is generated via coal gasification at the Great Plains Synfuel Plant, Beulah, ND, USA, and has a $\delta^{13}C$ of −20 to −21‰.[53] This is indistinguishable from the (wide) range of $\delta^{13}C$ for coal of −30 to −20‰ (Table 2). Data are not available for the coal and lignite used in the Synfuel plant, but coals and lignite from North Dakota have $\delta^{13}C$ between −25 and −23‰ with a minority of coal beds reaching −20‰.[54] The captured CO_2 from the Synfuel plant is thus at the ^{13}C-enriched end of the range of likely feedstock isotope values, consistent with our prior discussion.

3.3.2. Noble Gases. The noble gas composition of the captured CO_2 stream generated by gasification processes is likely to be controlled by the noble gas content of the feedstock and the steam and oxygen used in the gasification processes. Steam is likely to introduce noble gases that are a mixture of atmosphere and air saturated water (ASW) for the source water. Gasifiers that use partial oxidation rather than steam reforming will likely produce CO_2 enriched in heavy noble gases (Ar, Kr, and Xe) from added O_2.

3.4. Fermentation. Fermentation of biomass to produce ethanol as a sustainable fuel source is a well-developed industry in the USA and Brazil; while the total anthropogenic CO_2 emissions from bioethanol fermentation make up less than 1% of global CO_2 emissions, the CO_2 gas stream is of high purity and thus a suitable target for early adoption of CCS.[7] The two main crops used for bioethanol production are currently corn/maize (USA) and sugar cane (Brazil), both of which are C4 photosynthetic pathway plants.[55] Various other C4 crops, such as miscanthus switchgrass, and C3 plants, such as poplar,[56] are under investigation as suitable bioethanol feedstocks due to their ability to grow in relatively arid climates and their lack of economic competition as a food crop.[55] Ethanol is produced from the feedstock by fermentation of the sugars and starches in the biomass, generating a pure stream of CO_2 via[57]

DOI: 10.1021/acs.est.6b01548
Environ. Sci. Technol. 2016, 50, 7939−7955

$$C_6H_{12}O_6 \rightarrow 2C_2H_5OH + 2CO_2 \quad (1)$$

3.4.1. Carbon Isotopes. The carbon isotopic composition of plant sugars generally reflects the bulk plant composition; $\delta^{13}C$ of glucose from sugar beet (C3) is ∼−25.1‰[58] (cf. −30 to −24‰, Table 2) and from maize (C4) is $\delta^{13}C$ ∼ −10.5‰[58] (cf. −15 to −10‰, Table 2). Carbon isotopes are not evenly distributed within the glucose molecules and this results in fractionation of C-isotopes during fermentation;[58,59] the third and fourth carbon atoms in the glucose chain are enriched in ^{13}C relative to the bulk sugar, and these form the resulting CO_2.[59] Different degrees of ^{13}C enrichment of third and fourth position C atoms occur between C3 and C4 photosynthetic pathway plants, resulting in hypothetical ^{13}C enrichment of fermentation-produced CO_2 over glucose of ∼+8.2‰ for C3 plants and +4.5‰ for C4 plants.[59] Measured CO_2−glucose isotope fractionation factors range from +7.4 to +4.6‰ for C3 plants and +5.1‰ for C4 plants.[59−61] Apples are C3 plants and CO_2 produced during fermentation of cider has been measured with $\delta^{13}C$ of −25 to −21‰, which is enriched by at least 3‰ relative to C3 plants.[62]

Assuming that bioethanol feedstock will be dominated by C4 biomass and that CO_2 produced by fermentation is enriched in ^{13}C by 4−6‰ relative to the original sugars, we can expect CO_2 captured from fermentation plants to have $\delta^{13}C$ of ∼−11 to −4‰.

3.4.2. Noble Gases. The main source of noble gases during fermentation will be air saturated water (ASW) in the fermenting solution. Noble gases are more soluble in organic solvents, so we would expect solubility to increase as fermentation proceeds, resulting in noble gas depletion in the CO_2 stream.

3.5. Cement Industry. Cement production (including energy to drive the process and indirect emissions) contributes ∼6% of global anthropogenic CO_2 emissions, ∼50% of which is from calcination of limestone to produce lime and CO_2:[63,64]

$$CaCO_3(s) \rightarrow CaO(s) + CO_2(g) \quad (2)$$

The remaining emissions are from the energy required to fire the kiln; coal is commonly used but other fuels, such as natural gas, may be used. Likely carbon capture solutions for the cement industry include oxyfuel combustion to heat the kiln or amine capture for both kiln combustion and calcination gases.[63]

3.5.1. Carbon Isotopes. Calcination reactions are assumed to not cause isotopic fractionation, so the resulting CO_2 has the same isotopic composition as the initial carbonate[65,66]—i.e., $\delta^{13}C$ ∼ 0. Assuming a 50:50 mixture of CO_2 derived from calcination and from coal combustion, we would expect CO_2 emitted from cement factories to have $\delta^{13}C$ between ∼−11 and −16‰.

3.5.2. Noble Gases. Since the noble gas content of limestone is low (see Supporting Information section S.1.5), calcination of limestone is unlikely to significantly contribute noble gases to the CO_2 stream, which will be dominated by noble gases from fossil fuel combustion from firing the kiln.

3.6. Iron and Steel Industry. The steel industry generates 1.9 tonnes of CO_2 per tonne of steel[67] contributing 4−7% of global anthropogenic CO_2 emissions. CO_2 is generated from two processes: energy for steel production by burning of fuel and the use of reducing agents for steel production from iron ore, the most readily available reducing agent being coal.[67] Integrated steel plants (ISP) use mostly coal, with minor natural gas and oil, as both the fuel and reducing agent, while mini-mill plants use electric furnaces to heat and melt scrap or direct-reduced iron (DRI);[7] while mini-mill plants may not directly produce CO_2 emissions, DRI is produced by reacting iron ore with H_2 and CO to form iron + H_2O + CO_2.[7]

3.6.1. Carbon Isotopes. According to our investigations, there are no published data for carbon isotope fractionation between steel and CO_2; hence estimating $\delta^{13}C$ of CO_2 produced by integrated steel plants is difficult, but likely to be dominated by combustion CO_2 (so $\delta^{13}C$ of −31 to −21‰). In the case of DRI production an obvious source of H_2 and CO for the reduction process is Syngas. In this case, the $\delta^{13}C$ of CO_2 resulting from iron reduction would likely mirror that of the CO, as discussed for Syngas production (i.e., slightly depleted in ^{13}C relative to the gasification feedstock—section 3.3).

3.6.2. Noble Gases. The overall noble gas budget of CO_2 emitted from steel plants will be dominated by atmospheric noble gases incorporated during combustion, for integrated steel plants, and noble gases introduced during syngas production, for mini-mill plants. However, given the low concentration of He in air, enrichment of iron ore derived radiogenic ^4He may be significant.

3.7. CO_2 Separation. *3.7.1. Chemical Absorption.* Chemical absorption involves passing flue gases through a solvent with a high affinity for CO_2 (most commonly an amine solvent). In a typical amine capture process a CO_2-bearing flue gas is reacted with the amine solvent at ∼40 to 60 °C and the remaining flue gas (which will contain some residual CO_2) cleaned and vented; the CO_2-bearing solvent is transferred to a desorber vessel and heated to 100−140 °C to reverse the CO_2-binding chemical reaction and release a stream of pure (>99%) CO_2 gas.[7,68] Typical CO_2 recoveries are 80−95% of the CO_2 in the flue gas.[7] Such techniques are commonly employed to remove CO_2 from natural gas, before it is piped to national gas grids.[7] Various capture plants and aqueous amine solvents are being developed for chemical absorption of CO_2. The effects on inherent tracer composition will likely depend on the relative efficiencies of the absorption/desorption processes used by the capture process, the specific chemical reaction pathways that occur and the temperature and pH of the reactions. Two reaction pathways are common for amine solvents: bicarbonate (HCO_3^-) and carbamate ($NH_2CO_2^-$) formation.[68]

Carbon Isotopes. No data are yet available for C-isotope fractionation in the amine solutions commonly used in CO_2 capture. For water, C-isotope fractionation between CO_2 gas and bicarbonate is greater at lower temperatures.[27] In terms of carbon capture, this suggests that greater isotopic fractionation will take place during the absorption stage than the desorption stage. Below, we use Rayleigh Fractionation[27] to calculate expected $\delta^{13}C$ values for absorbed and desorbed CO_2.

In water at typical amine absorption temperatures (40−60 °C), the bicarbonate−CO_2 enrichment factor will be between +4 and +7‰.[27,69] If 85−99% of the CO_2 dissolves to form bicarbonate in the amine solution, the resulting bicarbonate will be enriched in ^{13}C by 0 to +2.34 ‰ relative to the original CO_2 flue gas. At desorption temperatures (100−140 °C), the HCO_3^-−CO_2 enrichment factor will be ±1‰,[69] and if 99% of the bicarbonate is desorbed, the resulting CO_2 will have a $\delta^{13}C$ value between −0.06 and +0.06‰ compared to that of the saturated bicarbonate. The net enrichment of captured CO_2 relative to original flue CO_2 will therefore be between −0.06 and +2.4 ‰, depending on the absorption and desorption temperatures.

DOI: 10.1021/acs.est.6b01548
Environ. Sci. Technol. 2016, 50, 7939−7955

An isotope fractionation factor of +1.011 (equivalent to an enrichment factor of ~ +11‰) has been determined for carbamate relative to aqueous CO_2.[70] ^{13}C enrichment between gaseous and aqueous CO_2 in fresh water at typical amine absorption temperatures (40−60 °C) is −0.9 to −1.0‰,[27] so the net isotope enrichment factor of carbamate relative to the original CO_2 flue gas will be ~+10‰. If 85−99% of the CO_2 dissolves to form carbamate in the amine solution, the resulting carbamate will be enriched in ^{13}C by +0.5 to +3‰ relative to the original flue gas CO_2. If 99% of the carbamate is desorbed, the resulting CO_2 will have $\delta^{13}C$ ~ 0.5‰ lower than the saturated carbamate, resulting in a net enrichment of ^{13}C in the captured CO_2 of 0 to +2.5‰ relative to the original flue gas.

The anticipated ^{13}C enrichment in CO_2 from amine capture, relative to the original flue gas CO_2, will be between −0.06 and +2.5‰, with the exact enrichment value dependent on absorption and desorption temperature, and the relative proportions of bicarbonate and carbamate species in the amine solution.

However, work investigating C-isotope fractionation during absorption of CO_2 by NH_3−NH_4Cl solutions at room temperature suggests that, in alkaline solutions, dissolved carbon (bicarbonate and carbamate ions) may be depleted in ^{13}C relative to the CO_2 gas by more than −50‰.[71] In the context of the above discussion regarding absorption/desorption efficiency, this may result in significant ^{13}C depletion in the captured CO_2 relative to the source gas, the opposite effect of what would be expected from dissolution in water.

The CO_2 injected at the Pembina CCS project was derived from the Ferus natural gas processing plant,[72] which presumably used a form of chemical absorption to strip CO_2 from natural gas. It had $\delta^{13}C$ ~ −4.7‰,[11] which falls well within the range of values for CO_2 coexisting with natural gas (−13.9 to +13.5,[73] Figure 1). Similarly, CO_2 captured using amine solvents from steam reforming of methane (see gasification, above) has $\delta^{13}C$ of −37‰,[50,52] well within the isotopic range of natural gas (−20 to −52‰). Given the breadth of possible $\delta^{13}C$ values for the source CO_2, these data do not help to constrain which of the above hypotheses is true, but suggest that ^{13}C enrichment of the captured CO_2 relative to the original CO_2 is less than ±20‰. More work to experimentally determine C-isotope fractionation during CO_2 capture would be beneficial. In the meantime, we tentatively conclude that fractionation of C-isotopes during amine capture is likely between −20 and +2.5‰ relative to the source CO_2, based on the available data for captured CO_2 relative to feedstocks, and the likely maximum enrichment calculated for CO_2 dissolution in fresh water.

Noble Gases. Few data are available for the noble gas content of the CO_2 stream produced by chemical absorption. In a summary of the CO_2 product stream specifications from a number of post-combustion capture technologies,[74] Ar was present at concentrations of 10−25 ppmv, much lower than the atmospheric concentration of 9340 ppmv (Table 1). This is likely due to the unreactive noble gases remaining in the gas phase during absorption and subsequently being vented, rather than being absorbed with the CO_2. A small proportion of the noble gases will dissolve into the amine solution. As noble gas solubility decreases with increasing temperature, these will be efficiently exsolved when the solvent is heated to release the CO_2. Noble gas solubility is controlled by Henry's Law with the heavy noble gases having greater solubilities than lighter noble gases. As a result we might expect noble gas element ratios to show heavy element enrichment relative to atmosphere.

3.7.2. Physical Absorption. Physical absorption of CO_2 requires a high partial pressure of CO_2 and is often used to separate CO_2 from other gases in CO_2-rich gas streams, such as the products of gasification processes. CO_2 absorption or dissolution into the solvent is according to Henry's Law.[75] No chemical reaction takes place, and the absorbed gas is released from the solvent by pressure reduction. Physical absorption using cold methanol is used to capture CO_2 produced at the Great Plains Synfuel plant, for use in the Weyburn enhanced oil recovery (EOR) and CCS site.[7]

Carbon Isotopes. To the best of our knowledge there are no data available to assess the effect of physical absorption on $\delta^{13}C$−CO_2. However, we would expect an enrichment of ^{13}C in the dense phase[27] (i.e., dissolved in the solvent) and the isotopic composition of the resulting captured CO_2 will depend on the relative efficiencies of the absorption and desorption mechanisms. If desorption is more efficient than absorption, then a small degree of ^{13}C enrichment is likely.

Noble Gases. In general, noble gases have a much higher solubility in organic solutions than in water[76,77] and follow Henry's Law, with the heavier noble gases having higher solubility. However, as is the case with noble gas dissolution in amine solvents, the noble gases will be preferentially retained in the gas phase and become decoupled from the CO_2. The small proportion of noble gases that are absorbed into the solvent will likely be enriched in the heavier noble gases relative to atmosphere due to the enhanced solubility of the heavier noble gases. Assuming efficient desorbing of gases from the physical solvent, CO_2 captured via physical absorption is likely to contain low concentrations of noble gases with element ratios enriched in heavy noble gases relative to the noble gas composition of the original flue gas. Isotopic ratios, however, are unlikely to change.

4. GEOCHEMISTRY OF FLUIDS AND GASES IN ACTUAL AND POTENTIAL CCS STORAGE SITES

The two types of storage sites currently considered to have the most potential for CCS in the short term are depleted oil and gas fields and deep, saline formations. In geological terms, these two types of storage are very similar, comprising reservoir rocks filled with saline fluid. In the case of depleted hydrocarbon fields, a wealth of information is available from hydrocarbon exploration and the fields are proven to have stored buoyant fluids or gas over geological time scales. On the other hand, many wells may have been drilled in such fields, resulting in potential leakage pathways, and many hydrocarbon fields are too small to provide large-scale CO_2 storage. Conversely, saline aquifers are much larger but are poorly studied due to lack of hydrocarbon accumulation, and it is not conclusively known whether a given aquifer is leak-tight with respect to buoyant fluids. Porous basalt formations pose another promising storage option,[78] but the chemical and transport processes involved in these cases have significant differences compared to storage in sedimentary formations and are beyond the scope of this review.

To trace CO_2 injected into a storage reservoir, the baseline conditions of the reservoir and the likely in-reservoir processes need to be known. Hydrodynamically closed reservoirs will tend to have more stable baseline conditions and predictable behavior, while hydrodynamically open reservoirs, and depleted hydrocarbon reservoirs that, at best will be contaminated with

DOI: 10.1021/acs.est.6b01548
Environ. Sci. Technol. 2016, 50, 7939−7955

drilling fluids and at worst may have been flushed with water to aid hydrocarbon recovery, may have spatially and temporally variable baselines, and thus exhibit less predictable behavior. Below we summarize the measured and expected geochemical baselines for potential storage reservoirs. While a reasonable amount of data is available for hydrocarbon reservoirs, less information is available for the baseline evolution after production ceases. Data for non-hydrocarbon-bearing saline aquifers are uncommon.

4.1. Carbon Isotopes. The $\delta^{13}C$ of CO_2 in storage formations generally varies between ∼−23 and +1‰ (Figure 2

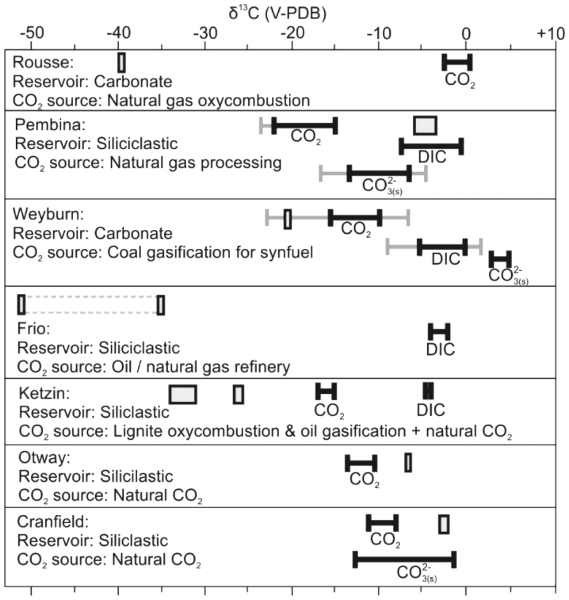

Figure 2. Baseline storage reservoir CO_2, DIC, and carbonate minerals, compared to injected CO_2 in existing CCS projects. Gray boxes show the $\delta^{13}C$ of injected CO_2; Frio and Ketzin show two boxes each to reflect the two anthropogenic CO_2 sources used in these projects. Reservoir baseline values for CO_2, DIC, and carbonate minerals are shown by horizontal crosshair lines. Where the baseline data are variable, the full range in values is shown by gray lines while the majority of reservoir data are represented by black lines. See Tables S2−S4 for references.

and Supporting Information Table S3). Formations that experience rapid flow of formation water or mixing of water reservoirs may exhibit a large range in $\delta^{13}C_{CO_2}$ values at a single site (e.g., −23 to −16‰ at Weyburn[79]). $\delta^{13}C$ for DIC are more constrained, based on the available data, and fall between −9 and +3‰ (see Supporting Information Table S3), regardless of whether the host rock is carbonate or siliciclastic, or whether the storage formation has experienced previous hydrocarbon exploitation, but this may reflect a limited data set. For storage reservoirs in depleted hydrocarbon fields or associated with EOR, the baseline isotope values may fluctuate strongly depending on industrial activities, such as water flushing[80] or contamination with organic matter resulting in enhanced bacterial action.[81]

4.2. Noble Gases. The most comprehensive noble gas measurements from a CCS reservoir are from the Weyburn EOR project,[82] although these do not represent baseline data. ^4He concentrations were 2 orders of magnitude greater than for air saturated water (ASW) while other noble gas isotopes (Ne − Kr) had concentrations 1−2 orders of magnitude lower. The isotopic composition of the noble gases is consistent with a depletion in atmospheric noble gases, as would be expected for a hydrocarbon-rich formation where the noble gases partition into the hydrocarbon phase, rather than the pore-water phase, and an enrichment in radiogenic isotopes, consistent with a deep origin of the fluid. Similarly at the Cranfield CO_2-EOR site, noble gas data from produced gases indicate high levels of terrigenic/radiogenic ^4He in the reservoir.[83] Other noble gas data are available for fluids from the Rousse and Frio storage reservoirs. The Frio data are restricted to He and Ar concentrations (80,000 ppb (≫air) and 400,000 ppb (≈ ASW) respectively[49]). Air-normalized concentrations for ^4He, ^{20}Ne, ^{36}Ar, ^{40}Ar and ^{84}Kr, from Rousse show that, while the concentration of ^4He was ∼10 times greater than air, the remaining noble gases were all 100−1000 times lower than air, with a positive correlation between concentration and elemental mass.[38]

These observations are consistent with the formation waters having interacted with hydrocarbons, causing depletion in atmospheric noble gases (originally derived via hydrologic recharge) relative to expected air saturated water (ASW), due to preferential partitioning into the hydrocarbon phase (section 2.2). Repeated dissolution and exsolution of noble gases will produce greater degrees of elemental fractionation, with an enrichment of heavy relative to light noble gases, compared to air.[84] While these processes facilitate precise quantitative modeling when all of the relevant conditions are well-characterized, it is difficult to place more quantitative constraints on the range of noble gas concentrations that could be expected in deep aquifers.

The isotopic composition of subsurface noble gas elements, however, does not fractionate during dissolution and exsolution and is instead controlled by mixing between different sources of noble gases. In very simplistic terms, the formations likely to be of most interest for CCS are those that have at least some degree of hydrodynamic isolation. In such cases, the fluids in the reservoir will be relatively old, residing in the subsurface for a considerable amount of time, perhaps approaching geological time scales. This will give a much stronger radiogenic and terrigenic noble gas signature than would be observed for shallow, freshwater aquifers that undergo regular recharge (see section 7). Noble gases in hydrocarbon systems often have a resolvable mantle component identified by elevated ^3He, and a high proportion of radiogenic isotopes that are often correlated with reservoir depth ($^4He^*$, $^{21}Ne^*$, and $^{40}Ar^*$, with "*" denoting a radiogenic origin).[30,85−87] Some hydrocarbon fields have elevated, isotopically atmospheric Kr and Xe that cannot be explained by elemental fractionation in a water−oil−gas system. This is attributed to adsorption of atmospheric Kr and Xe onto the carbon-rich sediments that are the source of hydrocarbons.[30,88] Such sediment derived Kr and Xe enrichments may occur in hydrocarbon fields, but would partition into the hydrocarbon phases, rather than water and so are unlikely to be observed in saline aquifers or depleted hydrocarbon fields where the Kr- and Xe-enriched phase was either never present or has been removed.

In the case of depleted oil and gas fields an additional source of noble gases may be introduced during water stimulation to maintain reservoir pressure. The extent of this contamination will depend on the relative volumes of water added, amount of original formation water remaining, and the noble gas composition of the injected water. If seawater is injected, as is likely in offshore hydrocarbon fields, the added noble gases

DOI: 10.1021/acs.est.6b01548
Environ. Sci. Technol. 2016, 50, 7939−7955

will be those of atmosphere equilibrated seawater (similar order of magnitude concentrations to those quoted for fresh water in Table 1). If produced fluids from the field are simply reinjected, then the noble gas composition is unlikely to change.

Many factors control the noble gas composition of potential storage reservoirs, so good noble gas baseline data will be beneficial if noble gases are to be used as tracers. Many reservoirs are likely to have elevated He concentrations relative to air or ASW and be depleted in other noble gases, while isotopic ratios will show strong radiogenic and terrigenic components. Saline aquifers will likely have more stable and consistent baselines than depleted hydrocarbon fields where contamination from production processes is likely.

5. GEOCHEMICAL EVOLUTION OF THE CO_2 STREAM ON INJECTION AND MIGRATION IN THE SUBSURFACE

Once injected into a geological storage formation, the fingerprint of the CO_2 stream will change depending on the processes and reactions that take place and the time scale and rate of those reactions. This section describes the changes that are likely to take place as the CO_2 plume migrates through the subsurface. Dominant processes will be mixing of the injected CO_2 with pre-existing materials, dissolution of the injected CO_2 into formation waters, fluid−rock reactions, such as dissolution of carbonate minerals, and migration. Precipitation of secondary carbonate and clay minerals will also change the stable isotope composition of the carbon-bearing gases and fluids in the subsurface, but there is currently limited evidence that these processes will occur on site-monitoring time scales, and, given the current uncertainties regarding mineral precipitation during CO_2 storage in sedimentary formations, these will not be considered here. Transport of CO_2 through the subsurface can be considered in terms of diffusive and advective transport, both of which may affect the composition of the CO_2 plume in different ways.

5.1. Carbon Isotopes. $\delta^{13}C$ evolution of injected CO_2 has been covered by a number of recent review papers[11,12,19,23−26] so is only qualitatively described here. Injected CO_2 will first mix with any free-phase CO_2 in the reservoir, resulting in a CO_2 plume with a $\delta^{13}C$ value resulting from mixing between injected and baseline values. Identification of the injected CO_2 plume is thus dependent on the difference between the injected and baseline $\delta^{13}C_{CO_2}$, the relative volumes of injected and baseline CO_2, and relevant enrichment factors (which in turn are dependent on temperature and salinity) between gases and dissolved C-species

CO_2 will begin to dissolve into the formation water to form dissolved inorganic carbon (DIC), with isotopic fractionation between CO_2 and DIC related to temperature, pH, and the DIC species formed. At reservoir conditions, DIC derived from the injected CO_2 is calculated to be enriched in ^{13}C by −1 to +7‰ relative to the coexisting CO_2.[27] This DIC will subsequently mix with baseline DIC.

Carbonic acid formation may cause dissolution of any carbonate minerals present, adding another source of C to the DIC; the stable isotope composition of these carbonate minerals, and thus resulting $\delta^{13}C_{DIC}$, depends on the origin of the carbonate (Figure 1).

Diffusive transport through rock or soil pore networks may cause C-isotope fractionation at the migration front, resulting in sequential ^{13}C depletion and then enrichment at a given location as the migration front passes.[12,89] For dry systems, if reactive mineral surfaces such as illite are present, $^{44}[CO_2]$-($^{12}C^{16}O_2$) may be preferentially adsorbed onto the surfaces, resulting in an initial ^{13}C enrichment of the free-phase CO_2, that can change the $\delta^{13}C_{CO_2}$ by up to hundreds of permil, followed by ^{12}C enrichment relative to the bulk CO_2 as the $^{12}CO_2$ is desorbed, resulting in lower $\delta^{13}C$ values, before returning to the bulk composition.[90] Further work is needed to investigate the presence of this effect in fluid saturated systems. While these processes are unlikely to affect the bulk of CO_2 injected for storage, they may affect the migration front of the injection plume and any CO_2 that leaks from the storage site. Early measurements of $\delta^{13}C_{DIC}$ at the Ketzin observation well Ktzi 200 gave $\delta^{13}C$ values lower than expected for mixing of CO_2 sources and calculated C-isotope fractionation during dissolution; diffusive fractionation was a speculated cause of this depletion.[81]

5.2. Noble Gases. The processes affecting noble gases in the subsurface are described in a number of recent summary papers and text books.[28−30,91,92] As with stable isotopes, the noble gas signature of the injected CO_2 stream will first be modified by mixing with any atmospheric, terrigenic, and radiogenic noble gas components in the reservoir gas phase. Exchange of noble gases between different reservoir phases (gas, water, oil, and solid particles) may take place according to the differences in solubility described in section 2.2. Note from Table 1 that Xe will partition preferentially into oil rather than gas at temperatures less than 50 °C so interaction of the injected CO_2 with any oil in the subsurface will cause Xe depletion in the gas phase. Recent work[93] experimentally determined noble gas partitioning between supercritical CO_2 and water and found deviations relative to ideal gas−water partitioning behavior that became greater with increasing CO_2 density. Ar, Kr, and Xe all show an increasing affinity for the CO_2 phase with increasing CO_2 density, due to enhanced molecular interactions of denser-phase CO_2 with the larger, more polarizable noble gases, while He shows decreasing affinity.[93]

Physical adsorption of noble gases onto solid particles, while difficult to quantify due to a lack of experimental data on adsorption properties, may significantly fractionate heavy from light noble gas elements, and a number of studies indicate enrichment of Kr and Xe in organic-rich shales and coal.[29,94,95]

Migration of the plume front may chromatographically fractionate the noble gas elements and CO_2 due to differences in molecular diffusion rate and solubility, although the specific manifestation of this fractionation depends on the rock matrix, the gas transportation mechanism, and relative solubility of the gas species. Less soluble species will migrate faster than more soluble species,[96] meaning that noble gases, which will preferentially partition into the gas phase, should travel faster through the subsurface than CO_2, which will begin to dissolve on contact with water. If gas transport takes place via molecular diffusion through pore space, the lighter, faster diffusing species will travel more quickly through the subsurface than the heavier, slower diffusing species. In the case of arrival of the migration front at a monitoring well, we would expect to detect gases in the following order, with the delay between gas arrival dependent on the distance traveled: He, Ne, Ar, CO_2, Kr, and Xe.[97] However, the opposite may be true when gas transport is via advection along fractures, with faster diffusing species, which are more able to enter the rock pore space, traveling less rapidly

DOI: 10.1021/acs.est.6b01548
Environ. Sci. Technol. 2016, 50, 7939−7955

than slower diffusing species, which are confined to fractures and more open, faster flow pathways.[98] The isotopic composition of the noble gases, however, is not expected to be altered by migration, so characterization of baseline and injected noble gas isotope compositions will allow mass-balance modeling and fingerprinting of any subsurface samples produced from monitoring wells.

6. PAST AND PRESENT USE AND FUTURE POTENTIAL OF INHERENT TRACERS FOR IN-RESERVOIR PROCESSES IN CCS PROJECTS

A number of projects have successfully used inherent stable isotopes to monitor CO_2 behavior in the subsurface, while added noble gases have also proven useful. Supporting Information Table S4 summarizes the ways that these tracers have been used in different CCS projects and identifies the key papers describing these applications. Many of these projects and applications have been summarized in recent review papers.[12,17,26]

Using C-isotopes as a CO_2 or DIC fingerprint to detect breakthrough and monitor migration of the injected CO_2 is the most common application of inherent tracers in existing CCS projects. In most of these projects the injected CO_2 was isotopically distinct from baseline CO_2 and DIC. However, C-isotopes were still a useful tool for monitoring migration and breakthrough at Weyburn, where the injected and baseline $\delta^{13}C_{CO_2}$ overlap (due to the wide range of baseline values), and at Pembina, where the injected $\delta^{13}C_{CO_2}$ overlapped with baseline $\delta^{13}C_{DIC}$ (Figure 2). In these cases, C-isotope fractionation during dissolution of injected CO_2 to form bicarbonate (~5‰ at 50−60 °C) increases the separation in $\delta^{13}C$ values between baseline DIC and injection derived HCO_3^-. In many cases (see Supporting Information Table S4), C-isotopes were the most sensitive tracer, indicating arrival of injected CO_2 at a monitoring well earlier than significant changes in fluid pH or CO_2 concentration. When the baseline conditions are well-characterized, C-isotopes have proven to be useful for quantifying the proportion of CO_2 or DIC derived from the injected CO_2 and from in-reservoir mineral dissolution (Weyburn,[12,99−101] Cranfield,[31] and Ketzin[81]). C-isotopes have also proven useful at identifying contamination from drilling fluids.[81]

Hence, $\delta^{13}C$ of CO_2 and DIC has the potential to be a powerful in-reservoir tracer, as long as the injected CO_2 has a $\delta^{13}C$ value that is easily distinguishable from background CO_2 and, if it dissolves, will produce DIC with $\delta^{13}C$ distinguishable from baseline DIC. Figure 3 compares the expected $\delta^{13}C$ of captured CO_2 from a number of processes and feedstocks, to the range of likely baseline storage formation values. From this, we can see that C3 biomass and fossil fuel derived CO_2 will be easiest to distinguish from reservoir baseline conditions, using $\delta^{13}C$, although coal and C3 biomass derived CO_2 have a greater chance of overlap.

While no studies have taken place using noble gases inherent to captured CO_2 as a tracer, use of noble gases coexisting with natural CO_2 injected for EOR operations[32] and as added tracers for both tracing CO_2 migration (Frio and Ketzin) and quantifying residual saturation (Otway) suggest that noble gases could prove very useful, if their injected composition is different from those of the reservoir baseline. In addition to experimental CCS sites, natural tracers have been used to study reservoir processes in natural CO_2 accumulations with

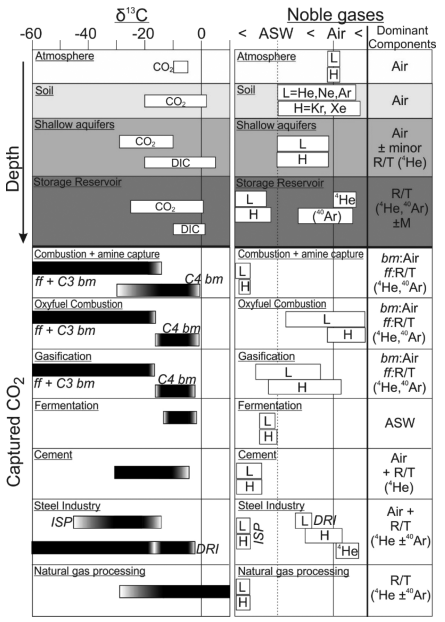

Figure 3. Comparison of the range of inherent tracer values for storage and leakage reservoirs (Table S1 and Tables S2−S6), and the expected captured CO_2 composition for various CO_2 sources (Table 2). Boxes represent the range of $\delta^{13}C$ (V-PDB) and noble gas concentration (relative to air and ASW) in baseline conditions for atmosphere, soil, shallow aquifers, and storage reservoirs, compared to the range of values expected for different sources of captured CO_2. C-isotopes are given in δ notation relative to V-PDB. Noble gases shown for absolute concentrations relative to air and ASW, with dominant components resolvable by isotopic analysis: "L" = light noble gases; "H" = heavy noble gases; "R/T" = radiogenic and/or terrigenic component; "M" = mantle component; "ASW" = air saturated water. ff = fossil fuels; bm = biomass; ISP = integrated steel plant; DRI = directly reduced iron.

combined noble gas and C-isotope measurements identifying CO_2 dissolution into the formation waters.[102]

7. BASELINE FINGERPRINT OF LEAKAGE PATHWAY RESERVOIRS (ATMOSPHERE, SOIL, AND GROUNDWATER AQUIFERS)

The aim of CCS is to prevent CO_2 from entering the atmosphere, so being able to detect seepage of geologically stored CO_2 to the atmosphere is a high priority. However, this remains difficult due to problems associated with identification of leakage sites, leakage plume dilution, and difficulties in establishing a precise local atmospheric baseline. In this section we will briefly review the probable range of baseline conditions for C-isotopes and noble gases in the reservoirs most likely to be influenced by CO_2 leakage and how these may or may not contrast with CO_2 leakage signatures.

7.1. Atmosphere. *Carbon Isotopes.* Atmospheric CO_2 has $\delta^{13}C$ of between −6 and −8‰ V-PDB[27] (Figure 1), but may vary spatially and temporally with local conditions, weather, and anthropogenic activity; e.g., atmospheric measurements in Dallas, TX, USA, ranged from $\delta^{13}C_{CO_2}$ of −12 to −8‰ over ~1.5 years due to varying photosynthetic uptake, respiration, and anthropogenic sources (vehicle emissions).[103] C-isotopes can be a sensitive tracer, despite large background fluctuations, by using Keeling plots, which correlate $\delta^{13}C_{CO_2}$ with inverse CO_2 concentration to determine the isotopic composition of local CO_2 (ecosystem respired and anthropogenic sources)

DOI: 10.1021/acs.est.6b01548
Environ. Sci. Technol. 2016, 50, 7939−7955

mixing with regional atmospheric CO_2.[104] If injected CO_2 were to leak to the atmosphere from the subsurface, it should be identifiable using Keeling plots as long as its $\delta^{13}C$ is different from that of the (previously established) baseline end members. Keeling plots from North and South America suggest that ecosystem respired CO_2 has $\delta^{13}C$ between −33 and −19‰,[104] which is similar to the anticipated $\delta^{13}C$ of CO_2 captured from burning C3 biomass and some fossil fuels; $\delta^{13}C$ of captured CO_2 may thus be especially difficult to distinguish from surface CO_2. Captured CO_2 derived from natural gas combustion may be depleted enough in ^{13}C and CO_2 captured from natural gas processing plants may be sufficiently enriched in ^{13}C to be distinguishable from local and regional atmospheric sources of $\delta^{13}C$.

Noble Gases. The concentration of noble gases in the atmosphere is given in Table 1. Atmospheric values for commonly used noble gas isotopic ratios include the following: $^3He/^4He = 1\ R/R_A$;[105] $^{20}Ne/^{22}Ne = 9.8$;[105] $^{40}Ar/^{36}Ar = 298.56$.[106] Regardless of the inherent noble gas composition of the injected CO_2 stream, if CO_2 leaks from deep geological storage, it will most likely be accompanied by baseline reservoir noble gases, which will be enriched in radiogenic and terrigenic isotopes (e.g., $^3He/^4He \ll 1\ R/R_A$; $^{40}Ar/^{36}Ar > 298.56$).

7.2. Soil. *Carbon Isotopes.* As with atmosphere, the stable isotope composition of soil CO_2 can vary spatially and temporally with local conditions. It is governed by a combination of CO_2 produced by soil respiration, fractionation during diffusion, mixing with atmospheric CO_2, and isotopic exchange with soil water.[89,107] This can result in highly variable $\delta^{13}C$ values for soil that vary on a daily basis. $\delta^{13}C$ data are available for soil from a number of CCS sites (Supporting Information Table S5), all of which show more than 10‰ variation (between −27 and −7‰) with no evidence of being contaminated by injected CO_2. There is considerable overlap between the $\delta^{13}C$ of soil CO_2 and the expected range of $\delta^{13}C$ values of captured CO_2 (Figure 3). CO_2 derived from combustion or gasification of natural gas may produce CO_2 significantly more depleted in ^{13}C than soil CO_2, while CO_2 captured from natural gas processing may be significantly enriched. Given the wide variation in baseline soil $\delta^{13}C$ values at any given site, C-isotopes in isolation will only be a useful leakage tracer if the leaking CO_2 has a distinctive $\delta^{13}C$ (i.e., derived from natural gas or natural gas processing), and if CO_2 concentration is also measured and Keeling plots are used. Use of $\delta^{13}C_{CO_2}$ in conjunction with concentrations of oxygen and nitrogen can be a useful tool to identify mixing between atmospheric CO_2 and CO_2 produced in the soil from biological respiration or methane oxidation.[108]

Noble Gases. In simplistic terms, noble gases in soil are derived from the atmosphere and partition between gas and water phases; soil gas should have an atmospheric noble gas composition, while fluids have concentrations consistent with air saturated water for the local soil temperature.[109] However, this ideal theoretical behavior is not always observed. Changes to the local combined partial pressure of CO_2 and O_2 (due to the greater solubility of CO_2 over O_2) can cause corresponding changes to noble gas concentrations and elemental ratios, with heavier noble gases more affected than lighter noble gases, likely due to differences in diffusion rate,[91] though isotopic ratios remain atmospheric. Three soil-gas monitoring projects associated with CCS sites provide limited noble gas concentration data (Supporting Information Table S5). At Weyburn, Ar concentrations[110] are atmospheric (~0.9%), and at Rousse, He concentrations from four separate campaigns were consistent at ~5 ppm,[111] again consistent with atmospheric concentrations. At Otway, baseline He concentrations in the soil ranged from 3 to 103 ppm,[112,113] i.e., ranging between enriched and slightly depleted compared to atmosphere. The reasons for these elevated He concentrations were unknown, but not thought to represent leakage of a deep gas source.

In terms of using noble gases to detect leaking CO_2, isotopic ratios will be the most useful tool. The isotopic ratios of noble gases in baseline soil will be atmospheric (see above), while noble gases in CO_2 leaking from depth will most likely have $^3He/^4He$ below atmospheric values, and $^{40}Ar/^{36}Ar$ greater than atmosphere, irrespective of the noble gas composition of the injected CO_2, due to enrichment of radiogenic $^4He^*$ and $^{40}Ar^*$ in the subsurface (see sections 2.2 and 4). Concentrations of noble gas elements or isotopes may provide additional information, depending on the noble gas content of the injected CO_2, and as long as variations in baseline soil noble gas partial pressure and elemental fractionation due to changing $CO_2 + O_2$ content are taken into account.

7.3. Shallow Aquifers. Shallow aquifers are often sources of potable water and hence CO_2 leakage into such reservoirs is undesirable. Such reservoirs are recharged by meteoric water and are thus hydrodynamically connected to the surface, so leakage of CO_2 into a shallow aquifer will likely result in escape of some of that CO_2 to the atmosphere. For these reasons, identification and mitigation of any CO_2 leakage into shallow aquifers will be a high priority.

Compared to the atmosphere or soil, baseline geochemical conditions in aquifers are likely to be much more stable, thus providing a higher sensitivity for leak detection. Furthermore, if the hydrodynamic gradient of an aquifer is well-characterized, monitoring wells can be placed downstream of any potential leakage structures, allowing efficient monitoring of a relatively large area without the need to identify and monitor every single potential leakage point.[114]

Carbon Isotopes. The $\delta^{13}C$ value of CO_2 and DIC in fresh spring and groundwaters is generally derived during recharge from the soil, followed by dissolution, associated isotope fractionation (see section 5) and weathering of carbonate material.[27] Bacterial action can isotopically enrich DIC in ^{13}C (up to +30‰), via reduction of CO_2 to methane (Figure 1), or fermentation of acetate to produce CH_4 and CO_2.[115−118]

Supporting Information Table S5 lists $\delta^{13}C$ for CO_2 and DIC in selected freshwater springs and aquifers. Data for Ketzin, Altmark, Otway, and Hontomín were collected as part of the CCS monitoring programs. $\delta^{13}C$ values of both CO_2 and DIC range from −24 to −9‰, consistent with derivation from soil CO_2 (Figure 1). Data from other aquifers extend the range to higher values, indicating bacterial action. $\delta^{13}C$ of CO_2 in shallow aquifers may be difficult to distinguish from $\delta^{13}C_{CO_2}$ of captured and injected CO_2, especially that derived from coal and biomass feedstocks and cement manufacture.

Noble Gases. Noble gases enter subsurface aquifers via recharge of meteoric water in the vadose zone of soils, and baseline compositions reflect ASW, with or without excess air, for the local soil temperature.[109] While deviations from this ideal behavior have been noted, these are most likely explained by changes to noble gas partial pressure in soil, described above.[91] In general, the processes that result in noble gas

DOI: 10.1021/acs.est.6b01548
Environ. Sci. Technol. 2016, 50, 7939−7955

elemental fractionation in meteoric and groundwater are controlled by well-understood physical mechanisms, are related to the residence time of water in the subsurface, and can be modeled.[33] Groundwater may thus provide a well-constrained, predictable baseline for leakage monitoring using noble gases. Furthermore, as noble gases are sparingly soluble in water, the concentration of noble gases in ASW is significantly lower than that of the atmosphere, resulting in a signal-to-noise ratio that is 100 times more sensitive.[119] While the processes controlling the noble gas content of groundwater are well-understood and their behavior predictable, they are dependent on specific local recharge conditions, so establishing a precise baseline is essential. As with atmospheric and soil reservoirs, the baseline of recently recharged aquifers is likely to differ from leaking CO_2 by a lack of radiogenic and terrigenic noble gases. However, old (hundreds of thousands of years) groundwaters may exist in aquifers used as domestic and agricultural water sources, and such aquifers may have significant radiogenic and terrigenic components. One such example is the Milk River aquifer in Alberta, Canada, which has groundwater residence times of up to 500 ka.[120] The majority of noble gases have concentrations between 0.2 and 4 times the expected values for ASW, but radiogenic and terrigenic derived ^4He is enriched in some wells by more than 2000 times the expected ASW value and $^{40}Ar/^{36}Ar$ values are all greater than atmosphere.[121]

8. PAST AND PRESENT USE AND FUTURE POTENTIAL OF INHERENT TRACERS FOR LEAK DETECTION IN CCS PROJECTS

Use of tracers for monitoring leakage of CO_2 into overlying reservoirs (aquifers, soil, and atmosphere) follows the same principles as for in-reservoir monitoring, but with the added complication that the released volumes are likely to be much smaller so sensitivity and detection become a critical issue.

Geochemical analysis is a common monitoring technique for CCS sites, many of which employ surface, soil, and/or groundwater analysis to monitor for leakage or contamination and a recent review[19] provides more details on the theory and practice of using tracers to detect CO_2 leakage into freshwater aquifers. However, in the vast majority of CCS field tests, no leakage has been observed and these projects are thus of limited value in assessing the viability of using inherent tracers as leakage detection. An exception is the Frio CCS project, where added tracers, elevated dissolved CO_2 gas contents, slight increases in HCO_3^- concentrations, and substantial depletion in ^{13}C of DIC were found in strata above a primary seal (but remaining below the main structural trap for the storage reservoir), indicating that CO_2 had leaked within the subsurface.[49] These indicators returned to background levels within 9 months of injection, suggesting that the leak was short-lived and occurred early in the injection process. Given that the injection well was 50 years old, leakage from the well itself was considered to be the most likely source of the CO_2, rather than migration between strata.[49] While it was not possible to calculate the volumes of leaked CO_2 at Frio, it seems that C-isotopes of DIC may provide a potentially powerful tracer of CO_2 leakage when volumes are so low that there is no significant rise in HCO_3^- concentration.

At the Rangely-Weber CO_2-EOR site, Colorado, USA, CO_2 and CH_4 gas fluxes were used to quantify microseepage from the reservoir.[122] Statistical analysis showed that gas flux and isotopic composition were different between the area overlying the reservoir and a nearby control site, but it was not possible to conclusively attribute these differences to gas seepage from the reservoir. Assuming that the differences were due to gas seepage, maximum seepage rates of 170 tonnes per year CO_2 and 400 tonnes per year CH_4 were calculated.[122]

Allegations of CO_2 leakage from the Weyburn EOR site into farmland (the Kerr Property) were shown to be unfounded,[123] but this case study provides useful insights of how natural tracers can help to determine the origin of CO_2, even when robust baseline data are not available. A number of incidents and CO_2 measurements led the owners of the farmland to believe that CO_2 injected into the Weyburn site was leaking into their property. One of the reasons for this belief highlights a potential downfall of using stable isotope data for tracing CO_2 migration; high concentrations of CO_2 measured in the soil had the same $\delta^{13}C_{CO_2}$ as the CO_2 being injected as part of the Weyburn project. This $\delta^{13}C_{CO_2}$ value (~−21‰) was, however, comparable to typical soil-gas CO_2 compositions[124] (cf. Figure 1). An independent investigation was commissioned to determine the origin of CO_2 on the site, the results of which showed without doubt that the CO_2 was natural and did not derive from injection of CO_2 for storage or EOR at Weyburn.[124] For soil gas, correlations of CO_2 with O_2 and N_2 were consistent with a CO_2 origin by soil respiration, rather than addition of an extra CO_2 component, and correlating CO_2 concentration with $\delta^{13}C_{CO_2}$ showed that the soil-gas isotope composition was easily explained by mixing between atmospheric CO_2 and soil-gas CO_2 with a $\delta^{13}C_{CO_2}$ of −25‰.[124] Noble gas and C-isotope analyses on groundwater well samples, injected CO_2 and water, and fluids produced from deep in the Weyburn formation confirmed that gas from the reservoir was not present.[82] Noble gas concentrations in the shallow groundwaters were consistent with ASW, as would be expected for the local groundwater system, while the fluids produced from the Weyburn field were very different; most noble gas concentrations (Ne, Ar, Kr, and Xe) in the Weyburn fluids were much lower than would be expected for ASW, while ^4He concentrations were much higher, consistent with enrichment of radiogenic ^4He in the crust.[82] Furthermore, $^3He/^4He$ ratios in groundwater samples were indistinguishable from air, while Weyburn fluids had $^3He/^4He$ values an order of magnitude lower, due to addition of crustal radiogenic ^4He.[82] Importantly, Weyburn reservoir water and shallow groundwater samples showed no correlation on a plot of HCO_3^- vs $^3He/^4He$, which would be expected if mixing occurred between deep, Weyburn fluids and ASW groundwater.[82]

In the absence of real CO_2 leaks from storage sites, information on tracer behavior during leakage can only be gleaned from controlled release experiments (i.e., injecting CO_2 into a unit that will leak) and studying natural CO_2 or natural gas seeps. Experiments releasing CO_2 into soil at a rate comparable to 0.001% leakage from a 200 Mt CO_2-storage site have been successful at identifying CO_2 leakage using $\delta^{13}C$ with Keeling plots in both atmosphere and soil, although in these cases the injected CO_2 had a particularly light isotopic signature ($\delta^{13}C$ ←45‰).[36,125−127] An experimental CO_2 leak ($\delta^{13}C_{CO_2}$ of −26.6‰) into sediments in the North Sea (QICS project) showed that $\delta^{13}C_{DIC}$ of pore water registered the leak earlier than significant increases in HCO_3^- concentration were detected.[128] In these examples the difference in $\delta^{13}C$ between baseline and injected CO_2 was 15−25‰. In these leakage experiments the migration distance for the injected CO_2 is

DOI: 10.1021/acs.est.6b01548
Environ. Sci. Technol. 2016, 50, 7939−7955

small (maximum 11 m − QICS), and it is possible that the isotopic composition of the CO_2 could change during migration over the larger distances associated with geological storage (kilometres deep). However, detailed modeling of potential leakage at the QUEST CCS project, Edmonton, Canada, from the Basal Cambrian Sandstone (BCS) storage reservoir into overlying aquifers indicated that the $\delta^{13}C_{CO_2}$ of the leaking CO_2 would differ from the injected CO_2 by less than 1‰.[52]

Another experiment released CO_2 with He and Kr tracers into the vadose zone of limestone and showed that molecular diffusivity was not an adequate model for coupled CO_2−tracer behavior; while He and Kr behaved according to predictive models, the CO_2 took significantly longer to travel through the substrate.[97] This experiment gives weight to the hypothesis that noble gases may provide an early warning of CO_2 leakage. Further evidence suggesting that noble gases may be useful tracers of CO_2 migration comes from studies on natural CO_2 and gas seeps. At St John's, Arizona/New Mexico, USA, $\delta^{13}C$ was inconclusive in establishing the origin of elevated HCO_3^- in spring water, but He and Ne isotopes identified both mantle and crustal components and thus a deep origin for the CO_2.[129] He and Ne isotopes were similarly used to confirm that elevated levels of soil-gas CO_2 and CH_4 were due to microseepage of gas from deep, hydrocarbon-bearing formations at Teapot Dome, Wyoming.[119] Importantly, this study established that total He concentrations of approximately just 10 ppm in soil gas and 0.1 ppm in groundwater aquifers would be sufficient to identify deep-sourced He.[119]

In summary, C-isotopes may be useful for detection of leakage and seepage if the baseline and injected CO_2 are significantly different. When isotopic compositions are not distinctive, combining $\delta^{13}C$ with CO_2, O_2, and N_2 concentrations can help to constrain the CO_2 origin. Of the noble gases, He is a particularly sensitive leak and seep tracer due to its low background concentrations at the surface and likely high concentration in the storage reservoir, regardless of the He content of the injected CO_2.

9. SUMMARY, IMPLICATIONS, AND CONCLUSIONS

The inherent stable isotope and noble gas composition of captured CO_2 has the potential to provide powerful monitoring tools for carbon capture and storage projects, both for in-reservoir processes and for identifying leakage and seepage from the storage unit. This application requires significant compositional differences between the injected CO_2 and the reservoir (for in-reservoir monitoring) and between the reservoir plus injected CO_2 and overlying shallow aquifers, soil, and atmosphere (for seepage monitoring).

In simplistic terms, captured CO_2 is generated in two stages: (1) initial reaction of a feedstock to produce a CO_2-bearing flue gas and (2) separation of the CO_2 from the other flue gases. When considering the likely isotopic and noble gas composition of the captured CO_2 stream, we found that the C-isotope composition and noble gas isotope ratios will be dominated by the initial feedstock, and noble gas concentrations will be controlled by the use of CO_2 purification technology.

For fossil fuel and C3 biomass feedstocks a $\delta^{13}C$ fractionation of −1.3‰ from the feedstock can be expected while the combustion of C4 biomass may result in greater isotope fractionation. There is a notable lack of information regarding the effect of CO_2 separation technologies (e.g., amine capture) on the stable isotope composition of captured CO_2, but ^{13}C depletion by tens of permil is hypothetically possible. Combining hypothetical considerations with the small amount of available data suggests that C-isotope fractionation during amine capture will be between −20 and +3‰. This amounts to a total fractionation between the feedstock and the captured CO_2 of between −21 and +2‰. A lack of solubility data for noble gases in amine solvents and a lack of detailed noble gas measurements on captured CO_2 makes it difficult to predict the noble gas content. Fossil fuel feedstocks are likely to be enriched in radiogenic or terrigenic noble gases (especially ^4He), and this isotopic component will be transferred to the CO_2, although any CO_2-purification processes are likely to cause noble gas depletion. However, there is a growing body of evidence to suggest that oxyfuel CO_2 (and other processes that use cryogenic oxygen, such as Syngas plants) may be enriched in heavy noble gases Kr and Xe. While fossil fuels remain the dominant feedstock, CO_2 captured from power plants will likely have a high ^4He content (at least before amine capture), but this will change over time if fossil fuels are increasingly replaced with biomass to provide renewable energy with potentially negative CO_2 emissions.

Likely baseline compositions for storage reservoirs and overlying aquifers, soil, and atmosphere were reviewed to assess the likelihood that injected CO_2 will be isotopically different, and this is summarized in Figure 3. Use of fossil fuels and C3 biomass feedstocks are most likely to produce captured CO_2 with $\delta^{13}C$ distinctive from baseline conditions, although $\delta^{13}C$ of the CO_2 in some storage reservoirs may be difficult to distinguish from coal or C3 biomass derived CO_2. CO_2 generated from C4 biomass, fermentation, cement manufacture, and natural gas processing will be more difficult to distinguish. Elevated ^4He concentrations that are expected to occur in various sources of captured CO_2 are unlikely to contrast with storage reservoir baseline conditions due to the presence of radiogenic and terrigenic ^4He, but may provide a highly sensitive tracer for detecting leakage and seepage. Elevated Kr and Xe in CO_2 captured from processes that use cryogenic oxygen may be useful, but there is not yet enough data to assess how ubiquitous this enrichment is and whether the concentrations involved are sufficient to allow detection in the reservoir. We note, however, that the wide range of noble gas element and isotope ratios that can be measured means that detailed baseline characterization of reservoir and injected CO_2 is likely to yield some combination of noble gas ratios that provide a suitable in-reservoir tracer.

A number of fundamental questions remain unanswered due to a lack of empirical data. While we have tried to address these questions hypothetically, more research is necessary to test these hypotheses. Specifically, (1) will carbon capture technologies result in low noble gas concentrations with preferential loss of light noble gases, and how much C-isotope fractionation will take place during carbon capture? (2) Will CO_2 captured from oxyfuel plants have a higher noble gas content than amine-captured CO_2, especially for heavy noble gases? (3) Will migration of the CO_2 plume over geological distances result in significant fractionation of stable isotopes or noble gases, over what time scales and distance will this fractionation be observed, and how might this affect our ability to identify CO_2 leakage or seepage?

DOI: 10.1021/acs.est.6b01548
Environ. Sci. Technol. 2016, 50, 7939−7955

■ ASSOCIATED CONTENT

Supporting Information

The Supporting Information is available free of charge on the ACS Publications website at DOI: 10.1021/acs.est.6b01548.

Information regarding feedstock composition and gasification processes (PDF)

Pivot table of $\delta^{13}C$ of various naturally occurring materials with data sources (XLSX)

■ AUTHOR INFORMATION

Corresponding Author

*Phone: +44 (0)131 6507010; fax: +44(0)131 6507340; email:sflude@gmail.com.

Notes

The authors declare no competing financial interest.

■ ACKNOWLEDGMENTS

This work was supported by EPSRC Grant No. EP/K036033/1. Editor Daniel Giammar and five anonymous reviewers are thanked for their comments and discussion.

■ REFERENCES

(1) Intergovernmental Panel on Climate Change. *Climate change 2013: The physical science basis*, Working Group I contribution to the fifth assessment report of the Intergovernmental Panel on Climate Change; Cambridge University Press: Cambridge, U.K., 2013.

(2) Intergovernmental Panel on Climate Change. *Climate change 2007: Mitigation*, Contribution of Working Group III to the fourth assessment report of the Intergovernmental Panel on Climate Change; Metz, B., Davidson, O. R., Bosch, P. R., Dave, R., Meyer, L. A., Eds.; Cambridge University Press: Cambridge, U.K., 2007.

(3) Intergovernmental Panel on Climate Change. Summary for policymakers and technical summary. *Climate change 2001: The scientific basis*, Working Group I report; Cambridge University Press: Cambridge, U.K., 2001.

(4) Intergovernmental Panel on Climate Change. Summary for policymakers and technical summary. *The Science of Climate Change*, Working Group I report; Cambridge University Press: Cambridge, U.K., 1996.

(5) *Energy technology perspectives 2014: Towards sustainable urban energy systems*, Executive Summary; International Energy Agency: Paris, 2014; 14 pp.

(6) Azar, C.; Johansson, D. J. A.; Mattsson, N. Meeting global temperature targets—the role of bioenergy with carbon capture and storage. *Environ. Res. Lett.* **2013**, *8* (3), 034004.

(7) *IPCC Special Report on Carbon Capture and Storage*; Metz, B., Davidson, O., de Coninck, H., Loos, M., Meyer, L., Eds.; Cambridge University Press: Cambridge, U.K., 2005.

(8) Pipitone, G.; Bolland, O. Power generation with CO_2 capture: Technology for CO2 purification. *Int. J. Greenhouse Gas Control* **2009**, *3* (5), 528−534.

(9) Aspelund, A.; Jordal, K. Gas conditioning—The interface between CO2 capture and transport. *Int. J. Greenhouse Gas Control* **2007**, *1* (3), 343−354.

(10) DIRECTIVE 2009/31/EC OF THE EUROPEAN PARLIAMENT AND OF THE COUNCIL of 23 April 2009 on the geological storage of carbon dioxide and amending Council Directive 85/337/EEC, European Parliament and Council Directives 2000/60/EC, 2001/80/EC, 2004/35/EC, 2006/12/EC, 2008/1/EC and Regulation (EC) No. 1013/2006. *Official Journal of the European Union*; European Parliament: Brussels, Belgium, 2009.

(11) Johnson, G.; Mayer, B.; Nightingale, M.; Shevalier, M.; Hutcheon, I. Using oxygen isotope ratios to quantitatively assess trapping mechanisms during CO_2 injection into geological reservoirs: The Pembina case study. *Chem. Geol.* **2011**, *283* (3−4), 185−193.

(12) Mayer, B.; Humez, P.; Becker, V.; Dalkhaa, C.; Rock, L.; Myrttinen, A.; Barth, J. A. C. Assessing the usefulness of the isotopic composition of CO_2 for leakage monitoring at CO2 storage sites: A review. *Int. J. Greenhouse Gas Control* **2015**, *37*, 46−60.

(13) White, D. J.; Hirsche, K.; Davis, T.; Hutcheon, I.; Adair, R.; Burrowes, S.; Graham, S.; Bencini, R.; Majer, E.; Maxwell, S. C. Theme 2: Prediction, monitoring and verification of CO_2 movements. In *IEA GHG Weyburn CO_2 Monitoring and Storage Project Summary Report 2000−2004*; Wilson, M., Monea, M., Eds.; Petroleum Technology Research Centre: Regina, Saskatchewan, Canada, 2004; Vol. *III*, pp 15−69.

(14) Bielicki, J. M.; Peters, C. A.; Fitts, J. P.; Wilson, E. J. An examination of geologic carbon sequestration policies in the context of leakage potential. *Int. J. Greenhouse Gas Control* **2015**, *37*, 61−75.

(15) *Monitoring, Verification, and Accounting of CO_2 Stored in Deep Geologic Formations*, DOE/NETL-311/081508; National Energy Technology Laboratory: Albany, OR, USA, 2009; 132 pp.

(16) Wells, A. W.; Diehl, J. R.; Bromhal, G.; Strazisar, B. R.; Wilson, T. H.; White, C. M. The use of tracers to assess leakage from the sequestration of CO2 in a depleted oil reservoir, New Mexico, USA. *Appl. Geochem.* **2007**, *22* (5), 996−1016.

(17) Myers, M.; Stalker, L.; Pejcic, B.; Ross, A. Tracers − Past, present and future applications in CO_2 geosequestration. *Appl. Geochem.* **2013**, *30*, 125−135.

(18) Nimz, G. J.; Hudson, G. B. The use of noble gas isotopes for monitoring leakage of geologically stored CO_2.. In *Carbon dioxide capture for storage in deep geologic formations—Results from the CO_2 capture project*; Vol. 2, Geologic storage of carbon dioxide with monitoring and verification; Thomas, D. C., Benson, S. M., Eds.; Elsevier: Thatcham, U.K., 2005; pp 1113−1128, DOI: 10.1016/B978-008044570-0/50152-5.

(19) Humez, P.; Lions, J.; Négrel, P.; Lagneau, V. CO_2 intrusion in freshwater aquifers: Review of geochemical tracers and monitoring tools, classical uses and innovative approaches. *Appl. Geochem.* **2014**, *46*, 95−108.

(20) Ljosland, E.; Bjørnstad, T.; Dugstad, Ø.; Hundere, I. Perfluorocarbon tracer studies at the Gullfaks field in the North Sea. *J. Pet. Sci. Eng.* **1993**, *10* (1), 27−38.

(21) Stalker, L.; Myers, M. Tracers − Pilot versus Commercial Scale Deployment for Carbon Storage. *Energy Procedia* **2014**, *63*, 4199−4208.

(22) Watson, T. B.; Sullivan, T. Feasibility of a Perfluorocarbon tracer based network to support Monitoring, Verification, and Accounting of Sequestered CO_2. *Environ. Sci. Technol.* **2012**, *46* (3), 1692−1699.

(23) Becker, V.; Myrttinen, A.; Blum, P.; van Geldern, R.; Barth, J. A. C. Predicting $\delta^{13}C_{DIC}$ dynamics in CCS: A scheme based on a review of inorganic carbon chemistry under elevated pressures and temperatures. *Int. J. Greenhouse Gas Control* **2011**, *5* (5), 1250−1258.

(24) Kharaka, Y. K.; Cole, D. R.; Thordsen, J. J.; Gans, K. D.; Thomas, R. B. Geochemical Monitoring for Potential Environmental Impacts of Geologic Sequestration of CO_2. *Rev. Mineral. Geochem.* **2013**, *77* (1), 399−430.

(25) Myrttinen, A.; Becker, V.; Barth, J. A. C. A review of methods used for equilibrium isotope fractionation investigations between dissolved inorganic carbon and CO_2. *Earth-Sci. Rev.* **2012**, *115* (3), 192−199.

(26) Nowak, M.; Myrttinen, A.; van Geldern, R.; Becker, V.; Mayer, B.; Barth, J. A. C. A brief overview of isotope measuremenets carried out at various CCS pilot sites worldwide. In *Clean Energy Systems in the Subsurface: Production, Storage and Conversion*; Hou, M. Z., Xie, H., Were, P., Eds.; Springer Series in Geomechanics and Geoengineering; Springer: Berlin, Heidelberg, 2013; pp 75−87, DOI: 10.1007/978-3-642-37849-2_7.

(27) Clark, I. D.; Fritz, P. *Environmental Isotopes in Hydrogeology*; CRC Press: Boca Raton, FL, USA, 1997.

(28) Aeschbach-Hertig, W.; Solomon, D. K. Noble Gas Thermometry in Groundwater Hydrology. In *The Noble Gases as Geochemical*

Tracers; Burnard, P., Ed.; Springer: Berlin, Heidelberg, 2013; pp 81−122, DOI: 10.1007/978-3-642-28836-4_5.
(29) Prinzhofer, A. Noble Gases in Oil and Gas Accumulations. In *The Noble Gases as Geochemical Tracers*; Burnard, P., Ed.; Springer: Berlin, Heidelberg, 2013; pp 225−247, DOI: 10.1007/978-3-642-28836-4_9.
(30) Ballentine, C. J.; Burgess, R.; Marty, B. Tracing Fluid Origin, Transport and Interaction in the Crust. *Rev. Mineral. Geochem.* **2002**, *47* (1), 539−614.
(31) Györe, D.; Stuart, F. M.; Gilfillan, S. M. V.; Waldron, S. Tracing injected CO_2 in the Cranfield enhanced oil recovery field (MS, USA) using He, Ne and Ar isotopes. *Int. J. Greenhouse Gas Control* **2015**, *42*, 554−561.
(32) Kipfer, R.; Aeschbach-Hertig, W.; Peeters, F.; Stute, M. Noble Gases in Lakes and Ground Waters. *Rev. Mineral. Geochem.* **2002**, *47* (1), 615−700.
(33) Widory, D. Combustibles, fuels and their combustion products: A view through carbon isotopes. *Combust. Theory Modell.* **2006**, *10* (5), 831−841.
(34) Warwick, P. D.; Ruppert, L. F. Carbon and oxygen isotopes of coal and carbon dioxide derived from laboratory coal combustion. *Int. J. Coal Geol.* **2016**, DOI: 10.1016/j.coal.2016.06.009.
(35) Moni, C.; Rasse, D. P. Detection of simulated leaks from geologically stored CO_2 with ^{13}C monitoring. *Int. J. Greenhouse Gas Control* **2014**, *26*, 61−68.
(36) Turekian, V. C.; Macko, S.; Ballentine, D.; Swap, R. J.; Garstang, M. Causes of bulk carbon and nitrogen isotopic fractionations in the products of vegetation burns: laboratory studies. *Chem. Geol.* **1998**, *152* (1−2), 181−192.
(37) Garcia, B.; Billiot, J. H.; Rouchon, V.; Mouronval, G.; Lescanne, M.; Lachet, V.; Aimard, N. A Geochemical Approach for Monitoring a CO_2 Pilot Site: Rousse, France. A Major gases, CO_2 -Carbon Isotopes and Noble Gases Combined Approach. *Oil Gas Sci. Technol.* **2012**, *67* (2), 341−353.
(38) Bhagavatula, A.; Huffman, G.; Shah, N.; Romanek, C.; Honaker, R. Source apportionment of carbon during gasification of coal−biomass blends using stable carbon isotope analysis. *Fuel Process. Technol.* **2014**, *128*, 83−93.
(39) Bottinga, Y. Calculated fractionation factors for carbon and hydrogen isotope exchange in the system calcite-carbon dioxide-graphite-methane-hydrogen-water vapor. *Geochim. Cosmochim. Acta* **1969**, *33* (1), 49−64.
(40) Brasseur, A.; Antenucci, D.; Bouquegneau, J.-M.; Coëme, A.; Dauby, P.; Létolle, R.; Mostade, M.; Pirlot, P.; Pirard, J.-P. Carbon stable isotope analysis as a tool for tracing temperature during the El Tremedal underground coal gasification at great depth. *Fuel* **2002**, *81* (1), 109−117.
(41) Richet, P.; Bottinga, Y.; Javoy, M. A Review of Hydrogen, Carbon, Nitrogen, Oxygen, Sulphur, and Chlorine Stable Isotope Fractionation Among Gaseous Molecules. *Annu. Rev. Earth Planet. Sci.* **1977**, *5* (1), 65−110.
(42) Dufaux, A.; Gaveau, B.; Letolle, R.; Mostade, M.; Noel, M.; Pirard, J. Modelling of the underground coal gasification process at Thulin on the basis of thermodynamic equilibria and isotopic measurements. *Fuel* **1990**, *69* (5), 624−632.
(43) Du, J.; Jin, Z.; Xie, H.; Bai, L.; Liu, W. Stable carbon isotope compositions of gaseous hydrocarbons produced from high pressure and high temperature pyrolysis of lignite. *Org. Geochem.* **2003**, *34* (1), 97−104.
(44) Shuai, Y.; Zhang, S.; Peng, P.; Zou, Y.; Yuan, X.; Liu, J. Occurrence of heavy carbon dioxide of organic origin: Evidence from confined dry pyrolysis of coal. *Chem. Geol.* **2013**, *358*, 54−60.
(45) Martens, S.; Kempka, T.; Liebscher, A.; Lüth, S.; Möller, F.; Myrttinen, A.; Norden, B.; Schmidt-Hattenberger, C.; Zimmer, M.; Kühn, M. Europe's longest-operating on-shore CO2 storage site at Ketzin, Germany: a progress report after three years of injection. *Environ. Earth Sci.* **2012**, *67* (2), 323−334.
(46) Nowak, M. E.; van Geldern, R.; Myrttinen, A.; Zimmer, M.; Barth, J. A. C. High-resolution stable carbon isotope monitoring indicates variable flow dynamic patterns in a deep saline aquifer at the Ketzin pilot site (Germany). *Appl. Geochem.* **2014**, *47*, 44−51.
(47) Hovorka, S. D.; Benson, S. M.; Doughty, C.; Freifeld, B. M.; Sakurai, S.; Daley, T. M.; Kharaka, Y. K.; Holtz, M. H.; Trautz, R. C.; Nance, H. S.; et al. Measuring permanence of CO2 storage in saline formations: the Frio experiment. *Environ. Geosci.* **2006**, *13* (2), 105−121.
(48) Kharaka, Y. K.; Thordsen, J. J.; Hovorka, S. D.; Seay Nance, H.; Cole, D. R.; Phelps, T. J.; Knauss, K. G. Potential environmental issues of CO2 storage in deep saline aquifers: Geochemical results from the Frio-I Brine Pilot test, Texas, USA. *Appl. Geochem.* **2009**, *24* (6), 1106−1112.
(49) Shell. http://www.shell.ca/en/aboutshell/our-business-tpkg/upstream/oil-sands/quest/technology.html. Accessed 2015.
(50) Olateju, B.; Kumar, A. Techno-economic assessment of hydrogen production from underground coal gasification (UCG) in Western Canada with carbon capture and sequestration (CCS) for upgrading bitumen from oil sands. *Appl. Energy* **2013**, *111*, 428−440.
(51) Shevalier, M.; Dalkhaa, C.; Humez, P.; Mayer, B.; Becker, V.; Nightingale, M.; Rock, L.; Zhang, G. Coupling of TOUGHREACT-Geochemist Workbench (GWB) for Modeling Changes in the Isotopic Composition of CO_2 Leaking from a CCS Storage Reservoir. *Energy Procedia* **2014**, *63*, 3751−3760.
(52) Mayer, B.; Shevalier, M.; Nightingale, M.; Kwon, J.-S.; Johnson, G.; Raistrick, M.; Hutcheon, I.; Perkins, E. Tracing the movement and the fate of injected CO_2 at the IEA GHG Weyburn-Midale CO_2 Monitoring and Storage project (Saskatchewan, Canada) using carbon isotope ratios. *Int. J. Greenhouse Gas Control* **2013**, *16*, S177−S184.
(53) Harrington, G. J.; Clechenko, E. R.; Clay Kelly, D. Palynology and organic-carbon isotope ratios across a terrestrial Palaeocene/Eocene boundary section in the Williston Basin, North Dakota, USA. *Palaeogeogr., Palaeoclimatol., Palaeoecol.* **2005**, *226* (3−4), 214−232.
(54) Koçar, G.; Civaş, N. An overview of biofuels from energy crops: Current status and future prospects. *Renewable Sustainable Energy Rev.* **2013**, *28*, 900−916.
(55) Sannigrahi, P.; Ragauskas, A. J.; Tuskan, G. A. Poplar as a feedstock for biofuels: A review of compositional characteristics. *Biofuels, Bioprod. Biorefin.* **2010**, *4* (2), 209−226.
(56) Xu, Y.; Isom, L.; Hanna, M. A. Adding value to carbon dioxide from ethanol fermentations. *Bioresour. Technol.* **2010**, *101* (10), 3311−3319.
(57) Rossmann, A.; Butzenlechner, M.; Schmidt, H.-L. Evidence for a Nonstatistical Carbon Isotope Distribution in Natural Glucose. *Plant Physiol.* **1991**, *96* (2), 609−614.
(58) Hobbie, E. A.; Werner, R. A. Intramolecular, compound-specific, and bulk carbon isotope patterns in C_3 and C_4 plants: A review and synthesis. *New Phytol.* **2004**, *161* (2), 371−385.
(59) Scrimgeour, C. M.; Bennet, W. M.; Connacher, A. A. A convenient method of screening glucose for13C:12C ratio for use in stable isotope tracer studies. *Biol. Mass Spectrom.* **1988**, *17* (4), 265−266.
(60) Weber, D.; Kexel, H.; Schmidt, H.-L. ^{13} C-Pattern of Natural Glycerol: Origin and Practical Importance. *J. Agric. Food Chem.* **1997**, *45* (6), 2042−2046.
(61) Cabañero, A. I.; Rupérez, M. Carbon isotopic characterization of cider CO_2 by isotope ratio mass spectrometry: a tool for quality and authenticity assessment: Carbon isotopic characterization of cider CO_2 by IRMS. *Rapid Commun. Mass Spectrom.* **2012**, *26* (16), 1753−1760.
(62) Ghoshal, S.; Zeman, F. Carbon dioxide (CO_2) capture and storage technology in the cement and concrete industry. In *Developments and Innovation in Carbon Dioxide (CO_2) Capture and Storage Technology*; Wood Head: Oxford, U.K., 2010; pp 469−491, DOI: 10.1533/9781845699574.5.469.
(63) Srivastava, R. K.; Vijay, S.; Torres, E. Reduction of Multi-pollutant Emissions from Industrial Sectors: The U.S. Cement Industry—A Case Study. In *Global Climate Change—The Technology Challenge*; Princiotta, F., Ed.; Springer: Dordrecht, The Netherlands, 2011; Vol. *38*, pp 241−272, DOI: 10.1007/978-90-481-3153-2_8.

(64) Andres, R. J.; Marland, G.; Boden, T.; Bischof, S. Carbon dioxide emissions from fossil fuel consumption and cement manufacture, 1751−1991 and an estimate of their isotopic composition and latitudinal distribution. In *The Carbon Cycle*; Wigley, T. M., Schimel, D. S., Eds.; Cambridge University Press, 1994.
(65) Andres, R. J.; Marland, G.; Boden, T.; Bischof, S. Carbon Dioxide Emissions from Fossil Fuel Consumption and Cement Manufacture, 1751−1991, and an Estimate of Their Isotopic Composition and Latitudinal Distribution. In *The Carbon Cycle*; Wigley, T. M. L., Schimel, D. S., Eds.; Cambridge University Press: Cambridge, 2000; pp 53−62.
(66) Birat, J.-P. Carbon dioxide (CO_2) capture and storage technology in the iron and steel industry. In *Developments and Innovation in Carbon Dioxide (CO_2) Capture and Storage Technology*; Maroto-Valer, M. M., Ed.; Wood Head: Oxford, U.K., 2010; pp 492−521, DOI: 10.1533/9781845699574.5.492.
(67) Lee, A. S.; Eslick, J. C.; Miller, D. C.; Kitchin, J. R. Comparisons of amine solvents for post-combustion CO_2 capture: A multi-objective analysis approach. *Int. J. Greenhouse Gas Control* **2013**, *18*, 68−74.
(68) Mook, W. G.; Bommerson, J. C.; Staverman, W. H. Carbon isotope fractionation between dissolved bicarbonate and gaseous carbon dioxide. *Earth Planet. Sci. Lett.* **1974**, *22* (2), 169−176.
(69) Tipton, P. A.; Cleland, W. W. Carbon-13 isotope effects on reactions involving carbamate and carbamoyl phosphate. *Arch. Biochem. Biophys.* **1988**, *260* (1), 273−276.
(70) Usdowski, E.; Hoefs, J. $^{13}C/^{12}C$ fractionation during the chemical absorption of CO_2 gas by the NH_3-NH_4Cl buffer. *Chem. Geol.: Isotope Geosci. Sect.* **1988**, *73* (1), 79−85.
(71) *Pembina Cardium "A" Lease—CO_2 Pilot Project Annual Report*; Penn West Energy Trust: Calgary, Alberta, Canada, 2006.
(72) Sheng, X.; Nakai, S.; Wakita, H.; Yongchang, X.; Wang, X. Carbon isotopes of hydrocarbons and carbon dioxide in natural gases in China. *J. Asian Earth Sci.* **1997**, *15* (1), 89−101.
(73) Abbas, Z.; Mezher, T.; Abu-Zahra, M. R. M. CO_2 purification. Part I: Purification requirement review and the selection of impurities deep removal technologies. *Int. J. Greenhouse Gas Control* **2013**, *16*, 324−334.
(74) Chen, W.-H.; Chen, S.-M.; Hung, C.-I. Carbon dioxide capture by single droplet using Selexol, Rectisol and water as absorbents: A theoretical approach. *Appl. Energy* **2013**, *111*, 731−741.
(75) Abrosimov, V. K.; Ivanov, E. V.; Lebedeva, E. Y. Solubility and Thermodynamics of Solvation of Krypton in Aqueous-Methanol Solutions of Urea at 101325 Pa and 278−318 K. *Russ. J. Gen. Chem.* **2005**, *75* (7), 1010−1016.
(76) Mainar, A. M.; Martínez-López, J. F.; Langa, E.; Pérez, E.; Pardo, J. I. Solubility of gases in fluoroorganic alcohols. Part II. Solubilities of noble gases in (water+1,1,1,3,3,3-hexafluoropropan-2-ol) at 298.15K and 101.33 kPa. *J. Chem. Thermodyn.* **2012**, *47*, 376−381.
(77) McGrail, B. P.; Schaef, H. T.; Ho, A. M.; Chien, Y.-J.; Dooley, J. J.; Davidson, C. L. Potential for carbon dioxide sequestration in flood basalts. *Journal of Geophysical Research: Solid Earth* **2006**, *111* (B12), B12201.
(78) Emberley, S.; Hutcheon, I.; Shevalier, M.; Durocher, K.; Gunter, W. D.; Perkins, E. H. Geochemical monitoring of fluid-rock interaction and CO2 storage at the Weyburn CO_2-injection enhanced oil recovery site, Saskatchewan, Canada. *Energy* **2004**, *29* (9−10), 1393−1401.
(79) Myrttinen, A.; Becker, V.; Nowak, M.; Zimmer, M.; Pilz, P.; Barth, J. A. C. Analyses of pre-injection reservoir data for stable carbon isotope trend predictions in CO_2 monitoring: preparing for CO2 injection. *Environ. Earth Sci.* **2012**, *67* (2), 473−479.
(80) Myrttinen, A.; Becker, V.; van Geldern, R.; Würdemann, H.; Morozova, D.; Zimmer, M.; Taubald, H.; Blum, P.; Barth, J. A. C. Carbon and oxygen isotope indications for CO_2 behaviour after injection: First results from the Ketzin site (Germany). *Int. J. Greenhouse Gas Control* **2010**, *4* (6), 1000−1006.
(81) Gilfillan, S. M. V.; Haszeldine, R. S. Report on noble gas, carbon stable isotope and HCO3 measurements from the Kerr Quarter and surrounding area, Goodwater, Saskatchewan. In *The Kerr Investigation Final Report: Findings of the investigation into the impact of CO_2 on the Kerr property*; Sherk, G. W., Ed.; IPAC CO_2 Research: Regina, Saschatchewan, Canada, 2011; pp 77−102.
(82) Gilfillan, S.; Haszedline, S.; Stuart, F.; Gyore, D.; Kilgallon, R.; Wilkinson, M. The application of noble gases and carbon stable isotopes in tracing the fate, migration and storage of CO_2. *Energy Procedia* **2014**, *63*, 4123−4133.
(83) Gilfillan, S. M. V.; Ballentine, C. J.; Holland, G.; Blagburn, D.; Lollar, B. S.; Stevens, S.; Schoell, M.; Cassidy, M. The noble gas geochemistry of natural CO_2 gas reservoirs from the Colorado Plateau and Rocky Mountain provinces, USA. *Geochim. Cosmochim. Acta* **2008**, *72* (4), 1174−1198.
(84) Ballentine, C. J.; O'Nions, R. K.; Oxburgh, E. R.; Horvath, F.; Deak, J. Rare gas constraints on hydrocarbon accumulation, crustal degassing and groundwater flow in the Pannonian Basin. *Earth Planet. Sci. Lett.* **1991**, *105* (1−3), 229−246.
(85) Ballentine, C. J.; O'Nions, R. K.; Coleman, M. L. A Magnus opus: Helium, neon, and argon isotopes in a North Sea oilfield. *Geochim. Cosmochim. Acta* **1996**, *60* (5), 831−849.
(86) Pinti, D. L.; Marty, B. *The origin of helium in deep sedimentary aquifers and the problem of dating very old groundwaters*; Special Publications; Geological Society: London, 1998; Vol. *144*, pp 53−68, DOI: 10.1144/GSL.SP.1998.144.01.05.
(87) Torgersen, T.; Kennedy, B. M. Air-Xe enrichments in Elk Hills oil field gases: role of water in migration and storage. *Earth Planet. Sci. Lett.* **1999**, *167* (3−4), 239−253.
(88) Stern, L.; Baisden, W. T.; Amundson, R. Processes controlling the oxygen isotope ratio of soil CO_2: analytic and numerical modeling. *Geochim. Cosmochim. Acta* **1999**, *63* (6), 799−814.
(89) Larson, T. E.; Breecker, D. O. Adsorption isotope effects for carbon dioxide from Illite- and quartz-packed column experiments. *Chem. Geol.* **2014**, *370*, 58−68.
(90) Freundt, F.; Schneider, T.; Aeschbach-Hertig, W. Response of noble gas partial pressures in soil air to oxygen depletion. *Chem. Geol.* **2013**, *339*, 283−290.
(91) Ozima, M.; Podosek, F. A. *Noble Gas Geochemistry*, 2nd ed.; Cambridge University Press: Cambridge, U.K., 2002.
(92) Warr, O.; Rochelle, C. A.; Masters, A.; Ballentine, C. J. Determining noble gas partitioning within a CO_2-H_2O system at elevated temperatures and pressures. *Geochim. Cosmochim. Acta* **2015**, *159*, 112−125.
(93) Bernatowicz, T. J.; Podosek, F. A.; Honda, M.; Kramer, F. E. The atmospheric inventory of xenon and noble gases in shales: the plastic bag experiment. *Journal of Geophysical Research* **1984**, *89* (B6), 4597.
(94) Podosek, F. A.; Bernatowicz, T. J.; Kramer, F. E. Adsorption of xenon and krypton on shales. *Geochim. Cosmochim. Acta* **1981**, *45* (12), 2401−2415.
(95) Bachu, S.; Bennion, D. B. Experimental assessment of brine and/or CO_2 leakage through well cements at reservoir conditions. *Int. J. Greenhouse Gas Control* **2009**, *3* (4), 494−501.
(96) Cohen, G.; Loisy, C.; Laveuf, C.; Le Roux, O.; Delaplace, P.; Magnier, C.; Rouchon, V.; Garcia, B.; Cerepi, A. The CO_2-Vadose project: Experimental study and modelling of CO_2 induced leakage and tracers associated in the carbonate vadose zone. *Int. J. Greenhouse Gas Control* **2013**, *14*, 128−140.
(97) Carrigan, C. R.; Heinle, R. A.; Hudson, G. B.; Nitao, J. J.; Zucca, J. J. Trace gas emissions on geological faults as indicators of underground nuclear testing. *Nature* **1996**, *382* (6591), 528−531.
(98) Emberley, S.; Hutcheon, I.; Shevalier, M.; Durocher, K.; Mayer, B.; Gunter, W. D.; Perkins, E. H. Monitoring of fluid−rock interaction and CO_2 storage through produced fluid sampling at the Weyburn CO_2-injection enhanced oil recovery site, Saskatchewan, Canada. *Appl. Geochem.* **2005**, *20* (6), 1131−1157.
(99) Raistrick, M.; Mayer, B.; Shevalier, M.; Perez, R. J.; Hutcheon, I.; Perkins, E.; Gunter, B. Using Chemical and Isotopic Data to Quantify Ionic Trapping of Injected Carbon Dioxide in Oil Field Brines. *Environ. Sci. Technol.* **2006**, *40* (21), 6744−6749.
(100) Shevalier, M.; Nightingale, M.; Johnson, G.; Mayer, B.; Perkins, E.; Hutcheon, I. Monitoring the reservoir geochemistry of the

DOI: 10.1021/acs.est.6b01548
Environ. Sci. Technol. 2016, 50, 7939−7955

Pembina Cardium CO_2 monitoring project, Drayton Valley, Alberta. *Energy Procedia* **2009**, *1* (1), 2095−2102.
(101) Lu, J.; Kharaka, Y. K.; Thordsen, J. J.; Horita, J.; Karamalidis, A.; Griffith, C.; Hakala, J. A.; Ambats, G.; Cole, D. R.; Phelps, T. J.; et al. CO_2−rock−brine interactions in Lower Tuscaloosa Formation at Cranfield CO_2 sequestration site, Mississippi, U.S.A. *Chem. Geol.* **2012**, *291*, 269−277.
(102) Gilfillan, S. M. V.; Lollar, B. S.; Holland, G.; Blagburn, D.; Stevens, S.; Schoell, M.; Cassidy, M.; Ding, Z.; Zhou, Z.; Lacrampe-Couloume, G.; et al. Solubility trapping in formation water as dominant CO2 sink in natural gas fields. *Nature* **2009**, *458* (7238), 614−618.
(103) Clark-Thorne, S. T.; Yapp, C. J. Stable carbon isotope constraints on mixing and mass balance of CO_2 in an urban atmosphere: Dallas metropolitan area, Texas, USA. *Appl. Geochem.* **2003**, *18* (1), 75−95.
(104) Pataki, D. E.; Ehleringer, J. R.; Flanagan, L. B.; Yakir, D.; Bowling, D. R.; Still, C. J.; Buchmann, N.; Kaplan, J. O.; Berry, J. A. The application and interpretation of Keeling plots in terrestrial carbon cycle research. *Global Biogeochemi. Cycles* **2003**, *17* (1), 1022.
(105) Porcelli, D.; Ballentine, C. J.; Wieler, R. An Overview of Noble Gas Geochemistry and Cosmochemistry. *Rev. Mineral. Geochem.* **2002**, *47* (1), 1−19.
(106) Lee, J.-Y.; Marti, K.; Severinghaus, J. P.; Kawamura, K.; Yoo, H.-S.; Lee, J. B.; Kim, J. S. A redetermination of the isotopic abundances of atmospheric Ar. *Geochim. Cosmochim. Acta* **2006**, *70* (17), 4507−4512.
(107) Amundson, R.; Stern, L.; Baisden, T.; Wang, Y. The isotopic composition of soil and soil-respired CO_2. *Geoderma* **1998**, *82* (1−3), 83−114.
(108) Romanak, K. D.; Bennett, P. C.; Yang, C.; Hovorka, S. D. Process-based approach to CO_2 leakage detection by vadose zone gas monitoring at geologic CO $_2$ storage sites. *Geophys. Res. Lett.* **2012**, *39* (15), L15405.
(109) Klump, S.; Tomonaga, Y.; Kienzler, P.; Kinzelbach, W.; Baumann, T.; Imboden, D. M.; Kipfer, R. Field experiments yield new insights into gas exchange and excess air formation in natural porous media. *Geochim. Cosmochim. Acta* **2007**, *71* (6), 1385−1397.
(110) Romanak, K. D.; Wolaver, B.; Yang, C.; Sherk, G. W.; Dale, J.; Dobeck, L. M.; Spangler, L. H. Process-based soil gas leakage assessment at the Kerr Farm: Comparison of results to leakage proxies at ZERT and Mt. Etna. *Int. J. Greenhouse Gas Control* **2014**, *30*, 42−57.
(111) Gal, F.; Michel, K.; Pokryszka, Z.; Lafortune, S.; Garcia, B.; Rouchon, V.; de Donato, P.; Pironon, J.; Barres, O.; Taquet, N.; et al. Study of the environmental variability of gaseous emanations over a CO_2 injection pilot—Application to the French Pyrenean foreland. *Int. J. Greenhouse Gas Control* **2014**, *21*, 177−190.
(112) Schacht, U.; Jenkins, C. Soil gas monitoring of the Otway Project demonstration site in SE Victoria, Australia. *Int. J. Greenhouse Gas Control* **2014**, *24*, 14−29.
(113) Schacht, U.; Regan, M.; Boreham, C.; Sharma, S. CO_2CRC Otway project−Soil gas baseline and assurance monitoring 2007−2010. *Energy Procedia* **2011**, *4*, 3346−3353.
(114) Carroll, S.; Hao, Y.; Aines, R. Geochemical detection of carbon dioxide in dilute aquifers. *Geochem. Trans.* **2009**, *10* (1), 4.
(115) Grossman, E. L.; Coffman, B. K.; Fritz, S. J.; Wada, H. Bacterial production of methane and its influence on ground-water chemistry in east-central Texas aquifers. *Geology* **1989**, *17* (6), 495.
(116) Hellings, L.; Van den Driessche, K.; Baeyens, W.; Keppens, E.; Dehairs, F. Origin and fate of dissolved inorganic carbon in interstitial waters of two freshwater intertidal areas: A case study of the Scheldt Estuary, Belgium. *Biogeochemistry* **2000**, *51* (2), 141−160.
(117) Sharma, S.; Frost, C. D. Tracing Coalbed Natural Gas−Coproduced Water Using Stable Isotopes of Carbon. *Groundwater* **2008**, *46* (2), 329−334.
(118) Simpkins, W. W.; Parkin, T. B. Hydrogeology and redox geochemistry of CH_4 in a Late Wisconsinan Till and Loess Sequence in central Iowa. *Water Resour. Res.* **1993**, *29* (11), 3643−3657.
(119) Mackintosh, S. J.; Ballentine, C. J. Using $^3He/^4He$ isotope ratios to identify the source of deep reservoir contributions to shallow fluids and soil gas. *Chem. Geol.* **2012**, *304*−*305*, 142−150.
(120) Hendry, J. M.; Schwartz, F. W.; Robertson, C. Hydrogeology and hydrochemistry of the Milk River aquifer system, Alberta, Canada: A review. *Appl. Geochem.* **1991**, *6* (4), 369−380.
(121) Andrews, J. N.; Drimmie, R. J.; Loosli, H. H.; Hendry, M. J. Dissolved gases in the Milk River aquifer, Alberta, Canada. *Appl. Geochem.* **1991**, *6* (4), 393−403.
(122) Klusman, R. W. Rate measurements and detection of gas microseepage to the atmosphere from an enhanced oil recovery/sequestration project, Rangely, Colorado, USA. *Appl. Geochem.* **2003**, *18* (12), 1825−1838.
(123) Sherk, G. W.; Romanak, K. D.; Dale, J.; Gilfillan, S. M. V.; Haszeldine, R. S.; Ringler, E. S.; Wolaver, B. D.; Yang, C. The Kerr Investigation: Final Report. Findings of the investigation into the impact of CO_2 on the Kerr Property; Sherk, G. W., Ed.;IPAC CO_2 Research: Regina, Saskatchewan, Canada, 2011.
(124) Romanak, K. D.; Changbing, Y. Analysis of gas geochemistry at the Kerr Site. In *The Kerr Investigation−Final Report. Findings of the investigation into the impact of CO_2 on the Kerr Property*; Sherk, G. W., Ed.; IPAC CO_2 Research: Regina, Saskatchewan, Canada, 2011; pp 57−76.
(125) Krevor, S.; Perrin, J.-C.; Esposito, A.; Rella, C.; Benson, S. Rapid detection and characterization of surface CO_2 leakage through the real-time measurement of $\delta 13\delta 13$ C signatures in CO_2 flux from the ground. *Int. J. Greenhouse Gas Control* **2010**, *4* (5), 811−815.
(126) McAlexander, I.; Rau, G. H.; Liem, J.; Owano, T.; Fellers, R.; Baer, D.; Gupta, M. Deployment of a Carbon Isotope Ratiometer for the Monitoring of CO_2 Sequestration Leakage. *Anal. Chem.* **2011**, *83* (16), 6223−6229.
(127) Spangler, L. H.; Dobeck, L. M.; Repasky, K. S.; Nehrir, A. R.; Humphries, S. D.; Barr, J. L.; Keith, C. J.; Shaw, J. A.; Rouse, J. H.; Cunningham, A. B.; et al. A shallow subsurface controlled release facility in Bozeman, Montana, USA, for testing near surface CO_2 detection techniques and transport models. *Environ. Earth Sci.* **2010**, *60* (2), 227−239.
(128) Blackford, J.; Stahl, H.; Bull, J. M.; Bergès, B. J. P.; Cevatoglu, M.; Lichtschlag, A.; Connelly, D.; James, R. H.; Kita, J.; Long, D.; et al. Detection and impacts of leakage from sub-seafloor deep geological carbon dioxide storage. *Nat. Clim. Change* **2014**, *4* (11), 1011−1016.
(129) Gilfillan, S. M. V.; Wilkinson, M.; Haszeldine, R. S.; Shipton, Z. K.; Nelson, S. T.; Poreda, R. J. He and Ne as tracers of natural CO_2 migration up a fault from a deep reservoir. *Int. J. Greenhouse Gas Control* **2011**, *5* (6), 1507−1516.
(130) Prinzhofer, A.; Dos Santos Neto, E. V.; Battani, A. Coupled use of carbon isotopes and noble gas isotopes in the Potiguar basin (Brazil): Fluids migration and mantle influence. *Mar. Pet. Geol.* **2010**, *27* (6), 1273−1284.
(131) Kotarba, M. J.; Nagao, K.; Karnkowski, P. H. Origin of gaseous hydrocarbons, noble gases, carbon dioxide and nitrogen in Carboniferous and Permian strata of the distal part of the Polish Basin: Geological and isotopic approach. *Chem. Geol.* **2014**, *383*, 164−179.

DOI: 10.1021/acs.est.6b01548
Environ. Sci. Technol. 2016, 50, 7939−7955